HHS Public Access

Author manuscript

Nat Med. Author manuscript; available in PMC 2023 November 01.

Published in final edited form as:

Nat Med. 2022 November ; 28(11): 2424–2435. doi:10.1038/s41591-022-02023-7.

Early intervention with 3BNC117 and romidepsin at antiretroviral treatment initiation in people with HIV-1: a phase 1b/2a, randomized trial

Jesper D. Gunst[1,2], **Marie H. Pahus**[1,2], **Miriam Rosás-Umbert**[1,2], **I-Na Lu**[3], **Thomas Benfield**[4], **Henrik Nielsen**[5,6], **Isik S. Johansen**[7], **Rajesh Mohey**[8], **Lars Østergaard**[1,2], **Vibeke Klastrup**[2], **Maryam Khan**[9,10], **Mariane H. Schleimann**[1,2], **Rikke Olesen**[1,2], **Henrik Støvring**[11], **Paul W. Denton**[12], **Natalie N. Kinloch**[13,14], **Dennis C. Copertino**[15,16], **Adam R. Ward**[15], **Winiffer D. Conce Alberto**[15,16], **Silke D. Nielsen**[1,2], **Maria C. Puertas**[17,18], **Victor Ramos**[19], **Jacqueline D. Reeves**[20], **Christos J. Petropoulos**[20], **Javier Martinez-Picado**[17,18,21,22], **Zabrina L. Brumme**[13,14], **R. Brad Jones**[15,16], **Julie Fox**[23,24], **Martin Tolstrup**[1,2], **Michel C. Nussenzweig**[19,25], **Marina Caskey**[19], **Sarah Fidler**[9,10], **Ole S. Søgaard**[1,2,Δ]

[1]Department of Clinical Medicine, Aarhus University, Aarhus, Denmark.

[2]Department of Infectious Diseases, Aarhus University Hospital, Aarhus, Denmark.

[3]Department of Neurology with Institute of Translational Neurology, University Hospital Münster, Münster, Germany.

[4]Department of Infectious Diseases, Copenhagen University Hospital - Amager and Hvidovre, Hvidovre, Denmark.

[5]Department of Infectious Diseases, Aalborg University Hospital, Aalborg, Denmark.

[6]Department of Clinical Medicine, Aalborg University, Aalborg, Denmark.

[7]Department of Infectious Diseases, Odense University Hospital, University of Southern Denmark, Odense, Denmark.

[8]Department of Internal Medicine, Regional Hospital Herning, Herning, Denmark.

[9]Department of Infectious Diseases, Imperial College Hospital, London, United Kingdom.

[10]The National Institute for Health Research, Imperial Biomedical Research Centre, London, United Kingdom.

[11]Department of Public Health, Aarhus University, Denmark.

[Δ]Corresponding author: Ole S. Søgaard, MD, PhD, Professor. olesoega@rm.dk.

Author Contributions Statement

OSS developed the trial design. JDG, MT, MCN, MC and OSS wrote the protocol. JDG, TB, HN, ISJ, RM, LØ, VK, JF, SF and OSS did the clinical visits. JDG, MHP, MRU, IL, MK, MS, RO, NNK, DCC, ARW, WDCA, SDN, MCP, JDR, CJP, JMP, ZLB, RBJ, MT and OSS did the laboratory assays and validations. VR performed the bioinformatic analysis. JDG, MHP, MRU and HS did the statistical analysis. JDG, PWD and OSS drafted the tables and figures. JDG and OSS drafted the article, which all authors critically revised for important intellectual content. JDG and OSS had full access to all the data in the study, verified the data, and had final responsibility for the decision to submit for publication.

Competing Interests Statement

MCN is listed as an inventor on patents for the antibody 3BNC117. JDR and CJP are employees of Labcorp-Monogram Biosciences. All other authors declare no competing interests.

[12]Department of Biology, University of Nebraska at Omaha, Omaha, Nebraska, United States of America.

[13]Faculty of Health Sciences, Simon Fraser University, Burnaby, British Columbia, Canada.

[14]British Columbia Centre for Excellence in HIV/AIDS, Vancouver, British Columbia, Canada.

[15]Infectious Diseases Division, Department of Medicine, Weill Cornell Medical College, New York, New York, United States of America.

[16]Department of Microbiology and Immunology, Weill Cornell Graduate School of Medical Sciences, New York, New York, United States of America.

[17]IrsiCaixa AIDS Research Institute, Badalona, Spain.

[18]CIBERINFEC, Madrid, Spain.

[19]Laboratory of Molecular Immunology, The Rockefeller University, New York, New York, United States of America.

[20]Labcorp-Monogram Biosciences, South San Francisco, California, United States of America.

[21]University of Vic–Central University of Catalonia, Vic, Spain.

[22]Catalan Institution for Research and Advanced Studies, Barcelona, Spain.

[23]Department of Genitourinary Medicine and Infectious Disease, Guys and St Thomas' National Health Service Trust, London, United Kingdom.

[24]Department of Genitourinary Medicine and Infectious Disease, The National Institute for Health Research Biomedical Research Centre, King's College London, London, United Kingdom.

[25]Howard Hughes Medical Institute, The Rockefeller University, New York, New York, United States of America.

Abstract

Attempts to reduce the HIV-1 reservoir and induce antiretroviral therapy (ART)-free virological control have largely been unsuccessful. In this phase 1b/2a, open-label, randomized controlled trial using a 4-group factorial design, we investigated whether early intervention in newly diagnosed people with HIV-1 with a monoclonal anti-HIV-1-CD4 binding-site antibody, 3BNC117, followed by a histone deacetylase inhibitor, romidepsin, shortly after ART initiation altered the course of HIV-1 infection [NCT03041012]. The trial was undertaken in five hospitals in Denmark and two hospitals in the United Kingdom. The co-primary endpoints were analysis of initial virus decay kinetics and changes in the frequency of CD4+ T cells containing intact HIV-1 provirus from baseline to day 365. Secondary endpoints included changes in the frequency of infected CD4+ T cells and virus-specific CD8+ T cell immunity from baseline to day 365, pre-ART plasma HIV-1 3BNC117-sensitivity, safety and tolerability, and time to loss of virologic control during a 12-week analytical ART interruption that started at day 400. Among 55 newly diagnosed people (5 females and 50 males) with HIV-1 who received random allocation treatment, we found that early 3BNC117 treatment with or without romidepsin enhanced plasma HIV-1 RNA decay rates compared to ART only. Further, 3BNC117 treatment accelerated clearance of infected cells compared to ART only. All groups had significant reductions in the frequency

of CD4+ T cells containing intact HIV-1 provirus. At day 365, early 3BNC117+romidepsin was associated with enhanced HIV-1 Gag-specific CD8+ T cell immunity compared to ART only. The observed virological and immunological effects of 3BNC117 were most pronounced in individuals whose pre-ART plasma HIV-1 envelope sequences were antibody-sensitive. The results were not disaggregated by sex. Adverse events were mild to moderate and similar between the groups. During a 12-week analytical ART interruption amongst 20 participants, 3BNC117-treated individuals harboring sensitive viruses were significantly more likely to maintain ART-free virologic control than other participants. We conclude that 3BNC117 at ART initiation enhanced elimination of plasma viruses and infected cells, enhanced HIV-1-specific CD8+ immunity and was associated with sustained ART-free virologic control among persons with 3BNC117-sensitive virus. These findings strongly support interventions administered at the time of ART initiation as a strategy to limit long-term HIV-1 persistence

Trial registration: clinicaltrials.gov identifier: NCT03041012.

Funding: The Danish Council for Independent Research (grants #7016-00022 and #9060-00023B), Central Region Denmark Research Fund, The Danish Regions' Medicine and Treatment Fund, Aarhus University, and Next Experimental Therapy Partnership.

INTRODUCTION

Upon human immunodeficiency virus type 1 (HIV-1) infection, integration of the viral genome into the DNA of immune cells establishes a long-lived HIV-1 reservoir. Cohort studies have shown that the integrated proviruses present during long-term antiretroviral therapy (ART) primarily consist of viruses that were circulating in plasma the year prior to ART initiation[1-5]. Due to the persistence of the HIV-1 reservoir, viral replication quickly resumes following ART interruption, leading to rebound of viremia within weeks in almost all individuals regardless of treatment duration[6-10]. Thus, life-long ART is currently necessary to suppress viral replication and prevent disease progression.

Until now, HIV-1 cure-related trials have almost exclusively focused on persons who have been on long-term suppressive ART. The "kick and kill" HIV-1 cure strategy aims at reducing or eliminating the viral reservoir by activating HIV-1 transcription and thus enabling immune-mediated killing of latently infected cells. Clinical trials testing latency-reversing agents (LRAs) such as histone deacetylase inhibitors (HDACi) have shown that viral transcription in latently infected cells can be (re)activated, but thus far no clinically meaningful reduction in viral reservoir size has been observed in humans[6,8,10-18]. Romidepsin (RMD) is one of the HDACi that in some clinical trials has been shown to induce HIV-1 expression in infected CD4+ T cells[19-21]. To boost HIV-1-specific immunity and enhance immune-mediated killing following latency reversal[22], therapeutic HIV-1 vaccines have been tested in combination with RMD. Two studies found that this combination strategy led to a modest decline in the HIV-1 reservoir, but no significant immune-mediated control of plasma viremia during a subsequent analytical treatment interruption (ATI)[9,23]. A third and larger randomized study found no impact on size of the viral reservoir when combining therapeutic HIV-1 vaccines with vorinostat, another HDACi[24].

A different potential strategy for enhancing HIV-1-specific immunity is through the administration of broadly neutralizing anti-HIV-1 antibodies (bNAbs) recognizing the HIV-1 envelope protein, gp120. In addition to direct neutralization of cell-free virus, bNAbs can also engage the immune system through their Fc domains and form antibody-antigen immune complexes[25-27]. These antibody-antigen immune complexes have been proposed to mediate a vaccinal effect that may lead to improved HIV-1-specific cellular immunity[28-32]. However, in long-term ART-treated individuals, levels of cell-free virus or HIV-1 envelope expression on infected cells may be too low to adequately engage Fc-mediated effector functions, and in two recent trials in ART-suppressed individuals, the bNAbs 3BNC117 and VRC07-523LS, each in combination with a HDACi, failed to reduce the intact HIV-1 reservoir size[10,33].

Interestingly, early treatment with bNAbs but not ART in simian/HIV (SHIV)$_{AD8\text{-}EO}$-infected non-human primates induced long-lasting HIV-1-specific immunity and durable immune-mediated control proposed to be at least in part due to SHIV-specific CD8+ T cells after the levels of bNAbs had waned[31,34]. In addition, a mathematical modelling study suggested that latency reversal at ART initiation may have a far greater impact on infected cells than latency reversal after years of ART due to ongoing immune activation[20,34-37].

Collectively, the lack of success of HIV-1 cure-related trials in long-term ART-treated individuals combined with the potential window of opportunity in newly diagnosed ART-naïve individuals as outlined above, led us to hypothesize that bNAbs with or without a LRA administered during ART initiation could potentially enhance the elimination of infected cells, reduce the size of the HIV-1 reservoir and improve HIV-1-specific T cell immunity. We conducted an investigator-initiated phase 1b/2a, open-label, multicenter, randomized controlled trial among individuals initiating ART to determine the safety and effects of 3BNC117 and/or RMD on decay of plasma viremia, dynamics of active HIV-1-infected cells, size of the HIV-1 reservoir, HIV-1-specific T-cell immunity, and duration of virologic control during a subsequent 12-week ATI (Fig. 1a).

RESULTS

Participants and follow-up

Eligible individuals were recruited from 16 January 2017 to 03 March 2020, and the last follow-up visit occurred on 17 July 2021. Of the total 60 participants enrolled in the study, 55 received the random allocation treatment (Fig. 1b, Extended Fig. 1). One participant was not randomized due to newly imposed national restrictions on non-COVID-19 research. Three other participants withdrew consent for personal reasons and did not receive the allocated treatment (one in the ART+RMD group and two in the ART+3BNC117+RMD group). One participant in the ART+3BNC117 group was taken out of the study due to hospital-admission with gram-negative bacteremia prior to receiving the first dose of 3BNC117. Of the remaining 55 (92%) participants, 15 were randomly allocated to the ART only group, 14 to the ART+3BNC117 group, 12 to the ART+RMD group, and 14 to the ART+3BNC117+RMD group. Two participants missed one of the three scheduled RMD infusions: one due to low neutrophil count (ART+RMD group) and one due to Influenza A infection (ART+3BNC117+RMD group). Three participants were lost to follow-up prior

to day 365 of whom two moved out of the study area (one in the ART+3BNC117 group and one in the ART+RMD group) and one participant had a relapse of psychiatric illness (ART+RMD group). The first administration of the two study drugs was spaced 7 to 10 days after ART initiation in order to distinguish the potential relatedness of adverse events to ART and the study drugs.

The four groups were overall well balanced (Table 1, Extended Table 1). Study participants were mainly (81%) Caucasian males and the median age was 36 years (interquartile range [IQR], 28–47 years). The proportion of participants with recent HIV-1 infection (<6 months from date of infection to study enrollment) ranged from 27% in the ART+3BNC117 group to 67% in the ART only group. Self-reported time of infection was confirmed by antibody-based recency testing (Extended Fig. 2). At baseline, the median CD4+ T cell count was 503 cells/mm^3 (range: 203–1,497) and the median plasma HIV-1 RNA level was 49,400 copies/mL (range: 730–24,000,000) for the total study population (Extended Table 1). Approximately half of the individuals (49%) had HIV-1 subtype B infection while the rest of the participants had a broad range of other HIV-1 subtypes and recombinant forms (Extended Table 1). Human leukocyte antigen (HLA) class I alleles known to be associated with rapid HIV-1 progression (i.e., B*07 and B*35) and elite control (i.e., B*27, B*57 and B*58) were represented in 44% of the participants across all 4 groups (Extended Table 1). Post-hoc bNAb-sensitivity testing of baseline plasma samples revealed that 8 of 15 (53%) participants in the ART+3BNC117 group and 10 of 16 (63%) in the ART+3BNC117+RMD had 3BNC117-sensitive plasma viruses at baseline (Fig. 2a). Notably, the individuals (n=18) harboring pre-ART 3BNC117-sensitive viruses were comparable to the individuals (n=13) harboring pre-ART 3BNC117-resistant viruses (Supplementary Table S1).

Decay rates of plasma HIV-1 RNA after ART initiation

Individuals with the lowest pre-ART plasma HIV-1 RNA levels were generally suppressed within 7 to 17 days after ART initiation, but not every individual had sustained viral suppression after 365 days of ART (Fig. 2b). To compare plasma viral load kinetics after ART initiation among the four groups, we split the decay rate of plasma HIV-1 RNA levels into three phases (Fig. 2c-d). During the 1st phase from the day of ART initiation to day 10, the median plasma HIV-1 RNA decay rates were comparable between the four groups. From day 10 to 24 of ART, the daily decay rate in median HIV-1 RNA was significantly faster for the ART+RMD+3BNC117 group with 16.9% (95%-confidence interval (CI): −27.3; −4.93%) compared to 10.0% (95%-CI: −14.9;−4.86%) in the ART only group (P = 0.048). The daily decay rate was also significantly faster for the ART+RMD group (median 18.5%, 95%-CI: −29.0; −6.51%; P = 0.017). From day 24 to day 90 of ART, the decay rates in median HIV-1 RNA levels were comparable between the groups. When both groups receiving 3BNC117 were analyzed according to 3BNC117-sensitivity, the daily percentage decay rates in median HIV-1 RNA were significantly faster among individuals with 3BNC117-sensitive viruses in both the ART+3BNC117 (P = 0.045) and the ART+RMD+3BNC117 (P = 0.042) groups compared to the ART only group from day 10 to 24 of ART (Fig. 2d). There was no significant difference in decay rates among individuals with 3BNC117-resistant viruses compared to the ART group (Fig. 2d). We conclude that 3BNC117 and RMD alone or in combination at ART initiation, led to faster 2nd phase

plasma HIV-1 RNA decay compared to ART alone, and that the effect of 3BNC117 was dependent on pre-ART plasma virus sensitivity to the bNAb.

Impact of 3BNC117 on active HIV-1-infeced cells

We next sought to determine if the faster decay in plasma viremia among 3BNC117-treated individuals was accompanied by enhanced elimination of infected cells. To this end, we used a single-cell RNA fluorescence in situ hybridization-flow cytometry (FISH-flow) assay to quantify HIV-1 transcriptionally and/or translationally active cells during the first 30 days of ART[38]. At baseline, the median number of CD3+CD8− T cells expressing either HIV-1 mRNA or Gag p24 protein or both per 10^6 cells in our study population was 180 (IQR: 150–230), 89 (IQR: 41–100) or 89 (IQR: 41–100), respectively. These measures of infected cells correlated with baseline plasma HIV-1 RNA, CD4+ T cell count and CD4/CD8 ratio (Supplementary Fig. S1a). There was no significant change in the number of CD3+CD8− T cells expressing p24 protein over the first 30 days in the ART only group (Fig. 3a), but a significant decrease in CD3+CD8− p24+ cells was observed in two groups: ART+3BNC117 (median 167, IQR: 62–359 cells; $P = 0.027$) and ART+RMD (median 80, IQR: 20–132 cells; $P = 0.031$) during the first 17 days of ART. Similar trends as those described above were observed for CD3+CD8-mRNA+ and CD3+CD8-mRNA+p24+ T cells (Extended Fig. 3).

To determine the immediate impact of the first 3BNC117 infusion (day 7) on HIV-1 transcription and/or translation, we analyzed the changes in infected cells within the first 10 days. Since both the ART only and ART+RMD groups only received ART during this period, we could combine data from the two groups and compare it to the combined data from the ART+3BNC117 and ART+3BNC117+RMD groups (Fig. 3b). We observed that the first administration of 3BNC117 led to a significant median fold decline in CD3+CD8-mRNA+ (0.45, IQR: 0.32–0.84; $P = 0.0078$) and CD3+CD8-mRNA+p24+ T cells (0.53, IQR: 0.33–0.69; $P = 0.0020$) (Fig. 3c-d). Similar reductions were observed for CD3+CD8−p24+ T cells (Fig. 3e, $P = 0.074$), where this decline was most pronounced among individuals with 3BNC117 pre-ART sensitive viruses (0.49, IQR: 0.20–0.97; $P = 0.027$). Individuals who only received ART did not have significant declines in the frequencies of HIV-1-infected cells (Fig. 3c-e). The 3BNC117-mediated decrease in HIV-1-infected cells during the first 10 days of ART was primarily driven by changes in the central memory CD3+CD8− T cells (Extended Fig. 4). We next used the viral protein spot (VIP-SPOT) to investigate the long-term effects of the interventions on HIV-1 p24+ cells[39]. The VIP-SPOT data correlated with baseline plasma HIV-1 RNA and level of intact proviruses (Supplementary Fig. S1b-c). While all four groups had a significant decrease in the median frequency of induced p24+ CD4+ T cells from baseline to day 365 (Extended Fig. 5a+b), we found that 47% of individuals with 3BNC117-sensitive viruses compared to 33% of individuals with 3BNC117-resistant viruses had no inducible p24+ CD4+ T cells at day 365 (Extended Fig. 5c). Collectively, these data demonstrate that 3BNC117 as adjunctive therapy to ART initiation enhanced clearance of HIV-1-infected cells and that this effect was greatest in the central memory compartment – a subset of CD4+ T cells believed to be important for HIV-1 persistence.

Effect of RMD on active HIV-1-infected cells

Before analyzing the 'per RMD' administration effects on HIV-1 transcriptional activity, we examined the impacts of RMD on CD3+CD8-p24+ cells specifically. Overall, we found a significant decrease in CD3+CD8-p24+ cells in the ART+RMD (median 32% reduction, IQR: 8%–70%; $P = 0.031$) group during the first 17 days of ART which persisted until day 30 (Fig. 3a, $P = 0.012$). Next, we analyzed changes in the frequency of CD3+CD8− T cells expressing either mRNA, p24 or both during RMD administration on day 10, 17 and 24 (Fig. 3f, Extended Fig. 6). When comparing each pre- to post-RMD infusion time point (1 week interval each), we observed significant median fold increases of 1.78 (IQR: 0.61–3.09; $P = 0.031$) in CD3+CD8-p24+ cells (Fig. 3g) and of 1.82 (IQR: 1.14–2.09; $P = 0.031$) in CD3+CD8-mRNA+p24+ after the first infusion, and of 1.40 (IQR: 1.08–1.93; P = 0.027) in CD3+CD8-mRNA+ after the third infusion (Extended Fig. 6). Collectively, the data show that RMD administration as latency reversing therapy during ART initiation modestly yet significantly boosted the number of transcriptionally and/or translationally active HIV-1-infected cells within 1 week of dosing, and this was associated with faster clearance of infected cells at later time points.

HIV-1 Gag-specific CD8+ T cell immunity

We used the activation-induced marker (AIM) assay to investigate HIV-1-specific T-cell responses. We noted that the median frequency of HIV-1 Gag-specific CD8+ T cells over 365 days of ART significantly declined in the ART only group, as expected following viral suppression/contraction phase of immunity. In contrast, the median frequency of HIV-1 Gag-specific CD8+ T cells remained stable over time in the three interventional groups. After 365 days of ART, the median frequency of HIV-1 Gag-specific CD8+ T cells in the ART+3BNC117+RMD group was higher than in the ART only group (0.95% vs 0.31%, respectively, $P = 0.011$) (Fig. 4a). When compared to the ART only group, the median frequency of HIV-1 Gag-specific CD8+ T cells on days 90 and 365 was significantly higher among the group that received 3BNC117 with or without RMD and whose pre-ART viruses were sensitive to 3BNC117 (Fig. 4b). Thus, 3BNC117 administration at ART initiation induces durable and potent HIV-1 Gag-specific CD8+ T cell immune responses.

Size of the HIV-1 reservoir

The droplet digital PCR (ddPCR)-based Intact Proviral DNA Assay (IPDA), which simultaneously targets the Packaging Signal (Ψ) and Rev Responsive Element (RRE) regions to identify genomically-intact proviruses, can be used to estimate reservoir size in people with HIV-1 subtype B. Since our study population feature both HIV-1 B and non-B subtypes, we performed an IPDA-like duplexed ddPCR (3dPCR) assay that targeted the same Ψ region as the published IPDA[40], and a region with the RRE, slightly downstream of the original IPDA target region, that has previously been used as a secondary location for this assay[41]. Where necessary, we adapted primer/probe sequences to accommodate HIV-1 polymorphisms (Supplementary Table S2). For 23 individuals who harbored HIV-1 B subtype and for whom sufficient sample was available, we additionally quantified intact proviruses using the published IPDA[40]. In line with a previous report[41], IPDA detection failure occurred in 6 (26%) of these 23 individuals, where polymorphism(s) were observed

in the IPDA probe(s) and/or at critical primer residue(s) in all cases (Supplementary Table S3). In the remaining 17 individuals however, the frequency of intact proviruses measured by IPDA correlated strongly with those measured by 3dPCR ($r = 0.89$, $P < 0.0001$; Supplementary Fig. S2), supporting 3dPCR as an accurate method to quantify intact proviral HIV-1 DNA. Using 3dPCR, we observed that the number of proviruses that were positive for both HIV regions, and thus presumed to be intact varied widely among individuals at baseline (range: 41–134,766 copies/10^6 CD4+ T cells, Extended Table 1), but did not differ between groups ($P = 0.68$) nor between HIV-1 B versus non-B subtypes ($P = 0.60$; Supplementary Fig. S3). At baseline, the level of intact proviruses correlated with frequency of induced p24+ CD4+ T cells, plasma HIV-1 RNA level and CD4+ T cell count (Supplementary Fig. S1c-e). All four treatment groups had a significant decrease in median intact and defective proviruses from baseline to day 365 (Fig. 4c, Extended Fig. 7). The largest median decreases in intact proviruses were observed among the three interventional groups, but there were no significant differences between the groups (Supplementary Table S4). Notably, the observed mean percentage reduction in the frequency of CD4+ T cells carrying intact provirus was greater for those whose pre-ART plasma viruses were sensitive to 3BNC117 compared to those that harbored resistant viruses (Fig. 4d).

ART interruption

To determine if the interventions had an impact on time to viral rebound, study participants were invited to participate in a closely monitored treatment interruption. Twenty individuals chose to participate in this optional 12-week ATI (Fig. 5a, Extended Fig. 1). The baseline characteristics of the ATI participants were comparable to those of the 35 non-ATI participants (Supplementary Table S5). The ATI started day 400 after ART initiation, which was over one year after the final 3BNC117 or RMD infusion. Seven of the 20 individuals did not reach criteria for viral rebound (defined as two consecutively measurements >5,000 copies/mL) and displayed partial ART-free virologic control with viremia ranging from <20–4,060 copies/mL at week 12 (Fig. 5A and Supplementary Table S6). Of these, one individual (id. 107) in the ART+3BNC117+RMD group had complete ART-free virologic control with undetectable plasma HIV-1 RNA throughout the 12 weeks (Fig. 5A and Supplementary Table S6). Among these seven individuals who all had negative plasma tests for antiretroviral drugs on day 84 of the ATI, two partial controllers had known protective HLA class I alleles: One individual in the ART only group (id. 707: HLA*B57, subtype CRF01 and pre-ART plasma HIV-1 RNA of 820 copies/mL) (Extended Table 1) and one individual in the ART+3BNC117+RMD group (id. 103: HLA*B27, subtype B, pre-ART plasma HIV-RNA of 730 copies/mL) (Extended Table 1). Moreover, of these seven individuals, five were enrolled less than 6 months from their presumed date of HIV-1 infection, which was corroborated by antibody-recency testing. To investigate whether the sensitivity of pre-ART plasma viruses to 3BNC117 affected time to loss of virologic control during ATI, we divided 3BNC117 recipients who underwent ATI (n=11) into 2 groups based on 3BNC117-sensitivity (Fig. 5b). Prior to ATI, individuals harboring pre-ART 3BNC117-sensitive versus those harboring 3BNC117-resistant viruses had non-significant higher frequency of HIV-1 Gag-specific CD8+ T cells and a trend towards lower levels of intact HIV-1 proviruses (Supplementary Table S1). Four of 5 (80%) individuals with 3BNC117 sensitive pre-ART plasma viruses had ART-free virologic control for 12 weeks,

while 0 of 6 (0%) individuals with pre-ART 3BNC117 resistant plasma viruses experienced ART-free virologic control (median 21 days to resuming ART, IQR: 21–35; $P = 0.0058$) (Fig. 5c). The one 3BNC117-sensitive individual who lost virologic control early on day 35 of the ATI (Fig. 5b), was HIV-1 seronegative at enrollment and had pre-ART plasma HIV-1 RNA level of 24,000,000 copies/mL (Extended Table 1). Since some of the ATI participants not receiving 3BNC117 also had partial ART-free virologic control, we compared 3BNC117 sensitive individuals to all other ATI participants but the difference in virologic control between the groups remained significant ($P = 0.025$) (Fig. 5d). Of note, no resistance mutations against 3BNC117 were identified in rebound viruses from baseline 3BNC117-sensitive individuals during the ATI (Supplementary Figure S5). Collectively, these findings demonstrate that adjunctive treatment with 3BNC117 at ART initiation led to a high rate of partial or complete ART-free virologic control during treatment interruption among 3BNC117-sensitive individuals more than a year after receiving the antibody.

Safety

Administration of 3BNC117 and/or RMD were safe and relatively well-tolerated. A total of 319 AEs were registered of which 205 AEs were determined to be unrelated to the study drugs (Extended Table 4). A total of 29 AEs, 27 grade 1 and two grade 2 were considered related to 3BNC117, with the most common AEs being fatigue (n=10) and headache (n=7). A total of 85 AEs of which 13 were grade 2, were considered related to RMD with nausea (n=32) and fatigue (n=21) being the most commonly reported. Six serious AEs were observed with none being related to either 3BNC117 or RMD (alanine transaminase increase [grade 3], bloodstream infection [grade 3], mental and behavioural disorder due to drug use [grade 2], pregnancy [grade 1], and relapse of psychiatric illness [grade 5]; Extended Table 4). The median CD4+ T cell count as well as CD4/CD8 ratio increased from baseline to day 365 in all the four groups during follow-up (Extended Fig. 8). Notably, the 13 participants who re-initiated ART during the ATI, rapidly achieved viral re-suppression (median 41 days, IQR: 28–56).

DISCUSSION

In this phase 1b/2a, open-label, multicenter, randomized controlled trial among newly diagnosed individuals initiating ART, we found that early 3BNC117 with or without RMD both enhanced the decay of plasma HIV-1 RNA and facilitated elimination of HIV-1-infected cells after ART initiation compared with ART-alone. We further demonstrated that the observed effects could be directly attributed to the ability of 3BNC117s fragment antigen-binding (Fab) region to bind to participants' unique viruses, as individuals harboring 3BNC117-sensitive viruses pre-ART, as predicted by pheno- or geno-typic assays, demonstrated significant changes in viral dynamics, HIV-1 specific immune responses and a higher frequency of virologic control following ART interruption. In the optional treatment interruption, four of 5 (80%) 3BNC117 recipients with pre-ART sensitive plasma viruses maintained ART-free virologic control throughout the 12 weeks of treatment interruption, compared to only 3 of 15 (20%) of those who either had pre-ART 3BNC117 resistant plasma viruses or who did not receive 3BNC117. We propose that the superior ART-free virologic control during the ATI amongst 3BNC117-sensitive individuals could be due to a

combination of early targeting of the proviral reservoir as well as enhanced cellular immune responses.

To our knowledge, no other HIV-1 curative interventions tested in a randomized trial have demonstrated faster decay in plasma viremia, decrease in the frequency of transcriptionally and/or translationally active HIV-1-infected cells and improved virus-specific cellular immunity associated with ART-free virologic control during ART interruption. Therefore, the findings presented in this study are encouraging for the field of HIV-1 cure research.

Of note, 3BNC117 has previously been administered to viremic individuals. A phase 1 trial showed that a single 3BNC117 (30 mg/kg) infusion reduced viremia by a mean of 1.5 $\log_{10}$ copies/mL among individuals who were not on ART[42]. In this study, as well as in other studies where bNAbs have been administered to ART naïve individuals, bNAb-sensitivity was essential for the antiviral efficacy[42-45]. Multiple studies have demonstrated that, in most individuals, circulating viruses developed resistance mutations within 1-3 weeks when bNAbs were administered at plasma viral loads above 10^4–10^5 copies/mL and participants were not on ART[42-45]. In our study, selection of resistance mutations against 3BNC117 was prevented by the co-administration of ART.

Interestingly, early 3BNC117 treatment with or without RMD enhanced elimination of HIV-1-infected cells during the 1st phase as well as decay of plasma HIV-1 RNA in the 2nd phase following ART initiation among 3BNC117-sensitive individuals. Integrase-inhibitor based triple ART regimens are extremely effective at suppressing plasma viremia in ART naïve individuals, and multiple clinical trials investigating 4- or 5-drug ART intensification regimens have failed to enhance the suppression of initial viremia compared to integrase-inhibitor based triple ART alone[46,47]. Thus, it appears that 3BNC117 may mediate its antiviral effects through different mechanisms than regular small molecule antiretroviral drugs. Multiple *in vitro* and *in vivo* studies have documented bNAbs' ability to directly neutralize cell-free virus across several HIV-1 subtypes[48,49]. In addition, *in vitro* and animal experiments indicate that 3BNC117 can enhance clearance of HIV-1-infected cells though Fc-mediated effector functions[26,50-52]. While it could be argued that the latter effect might primarily target short-lived productively infected cells and not long-term HIV-1 persistence[27,53], we were able to demonstrate that 3BNC117 mainly eliminated infected cells in the central memory subset – a subset shown to be the main T cell compartment harboring the latent replication-competent HIV-1 reservoir during long-term ART[54-57]. Thus, we conclude that potent bNAbs like 3BNC117 can enhance elimination of cell-free virus and infected cells among individuals initiating ART through biological mechanisms that differ from standard antiretroviral drugs.

Antigen-antibody complexes can form when bNAbs bind to cell-free HIV-1 virus or antigen on the surface of infected cells[27]. These immune complexes stimulate antigen uptake and presentation by antigen-presenting cells in lymphoid tissues leading to T cell cross-presentation and augmented adaptive HIV-1-specific CD8+ T cell responses[25]. This antibody-mediated vaccinal effect likely requires substantial immune complex formation and thus, an abundance of antigen, which may be why enhancement of HIV-1-specific immunity has not been observed among long-term suppressed individuals who receive

bNAbs in addition to ART[10]. In our study, HIV-1-specific CD8+ T cell responses were enhanced among 3BNC117-sensitive individuals receiving early 3BNC117 with or without RMD. This maintenance of HIV-1 specific CD8+ T cell responses after ART initiation might be particularly important to achieve some degree of post-treatment control, as strong CD8+ T cell immunity has been linked to HIV-1 remission in non-human primates and elite controllers[29,31,58]. Further, another recent study demonstrated that maintenance of HIV-1-specific CD8+ cell responses was directly correlated to the sensitivity of pre-ART plasma viruses to 3BNC117 neutralization (unpublished manuscript by Rosas-Umbert M. et al.). This may explain why circulating autologous non-neutralizing or low-affinity antibodies do not the same pleiotropic effect on CD8+ T cells as observed following administration of high-titer potent bNAbs. Of note, increased HIV-1 specific CD8+ T cell responses have also been observed after administration of two bNAbs 2 days prior to and into an ART interruption[29,59]. Thus, our findings suggest that adding bNAbs at ART initiation when plasma viral loads are high might be an effective means of directing and enhancing an individual's CD8+ T cell immune responses against autologous viruses through immune-complex formation and other Fc-mediated effector functions. Whether the higher HIV-1-specific CD8+ T cell responses observed 1 year after starting ART among bNAb-sensitive individuals receiving early 3BNC117 was caused by higher peak responses, protracted CD8+ T cell memory contraction, or other factors may be explored in future trials.

In this report, we focused primarily on the effect of 3BNC117 with or without RMD administration to ART initiation, but the effectiveness of RMD and other pan-HDACi as LRAs have varied considerably between studies. Our study is the first in which an HDACi has been administered during ART initiation. Consistent with a number of prior studies in long-term ART-treated individuals, we observed modest increases in HIV-1 mRNA and/or p24 expression, from pre- to post-infusion suggesting that RMD induced HIV-1 expression in infected cells[9-11,21,23]. Additionally, early RMD at ART initiation also led to a faster median daily decay of plasma HIV-1 RNA during the 2nd phase and enhanced clearance of translationally active HIV-1-infected cells during the first 30 days of ART, indicating that early latency reversal can affect the viral reservoir[20,34-37]. However, the ART+RMD group did not experience a delay in time to viral rebound during the ATI and therefore, the clinical benefit of LRAs at ART initiation, without adding an immunological agent that enhances killing of infected cells, remains uncertain[60].

Our study also has some limitations and may not be generalizable to all newly diagnosed individuals due to the study's stringent exclusion criteria. For instance, during screening we excluded 25% of the newly diagnosed individuals due to CD4+ T cell counts <200 cells/mm^3. Less than 50% of the randomized participants underwent ATI but importantly, the characteristics of those who interrupted ART were not different from those who did not interrupt ART suggesting that outcomes observed among ATI participants were likely generalizable to the total study population. Additionally, our analyses were done on peripheral blood but it would be of great interest to compare these findings to complementary analyses performed on tissue samples, e.g. lymphatic tissues[61] in future studies. Finally, the findings from this clinical study needs to be verified in larger scale both to increase generalizability as well as statistical power.

In conclusion, our findings suggest that administration of 3BNC117 at the time of ART initiation reduced the number of transcriptionally active HIV-1-infected cells, resulted in a faster decay of plasma HIV-1 RNA, and increased HIV-1 CD8+ T cell immunity, compared to ART alone. Our findings are consistent with the observation that bNAb administration during ART interruption may accelerate reservoir decay[62]. Importantly, co-administration of 3BNC117 with or without RMD to ART initiation led to prolonged ART-free virologic control during treatment interruption in a subset of individuals whose pre-ART viruses were sensitive to the bNAb. Collectively, the findings strongly support the further development of interventions administered at the time of ART initiation as a strategy to limit long-term HIV-1 persistence.

METHODS

Study design

This was a phase 1b/2a, open-label, multicenter, randomized controlled trial enrolling at five sites in Denmark and two sites in the United Kingdom. Prior to any study-related procedures, written informed consent was obtained from the participant. Participants were randomized into one of four groups: ART only, ART+3BNC117, ART+RMD, or ART+3BNC117+RMD in a 1:1:1:1 ratio (Fig. 1a+b). Screening occurred within 4 weeks prior to the baseline visit at day 0. Participants were followed until day 365 of ART or longer if they chose to enroll in the optional 12-week ATI at day 400. The study was conducted in accordance with Good Clinical Practice and reported in accordance with the CONSORT 2010 statement[63]. The protocol was approved by the Danish Medicine Authorities in Denmark and the Medicines (#2016053184) and Healthcare Products Regulatory Agency (MHRA) in the United Kingdom (#31883/0001/001-0001), and the National Committee on Health Research Ethics in Denmark (#1-10-72-110-16) and National Health Authority in the United Kingdom (#241439). Study data were collected and managed in Research Electronic Data Capture (REDCap) electronic data capture tools hosted at the Clinical Trial Unit, Department of Clinical Medicine, Aarhus University, Aarhus, Denmark[64,65]. The study was monitored by the Danish Good Clinical Practice Units (https://gcp-enhed.dk/english/) from screening to final visit.

Participants

Newly-diagnosed ART naïve participants aged 18-65 years with a confirmed HIV-1 diagnosis and a CD4+ T cell count >200 cells/mm^3 at screening were recruited by study physicians. All participants initially received integrase inhibitor-based ART regimens. Participants were reimbursed for transport expenses relating to the study, but otherwise did not receive any financial compensation for participating in the study except from compensation for lost earnings during study visits. Detailed inclusion and exclusion criteria can be found in the protocol: eCLEAR-001, version 3.1, 18 September 2018.

Randomization

The Clinical Trial Unit at Aarhus University generated the randomization sequence using permuted blocks of 4 or 8 by computer-generated random numbers without stratification to sex and age. Randomization assignment was provided to each site through using REDCap.

Procedures

3BNC117 was administered intravenously at a dose of 30 mg/kg over 60 min at day 7±3 and 21±3 after ART initiation. 3BNC117 dosing was based on previously observed antiviral efficacy in clinical studies[42,59,66]. RMD (Bristol Myers Squibb) at 5 mg/m^2 was administered intravenously over 120 min at day 10±3, 14±3 and 24±3 after ART initiation. RMD dosing was based on previously observed latency reversal in clinical studies[9,11,23]. Study participants were monitored with vital signs prior to, during, and for 1 hour after each infusion. Pre-medication with ondansetron 8 mg orally was offered as prophylactic antiemetic treatment at least 30 min prior to each RMD infusion. The infusion visits were in Denmark completed at the Clinical Research Units, Aarhus University Hospital or Hvidovre Hospital and in United Kingdom done at the National Institute for Health Research, Imperial Clinical Research Facility or the Clinical Research Facility, Guy's and St Thomas' Biomedical Research Centre. Follow-up visits were completed at the respective outpatient clinics of participating hospitals. Blood samples were collected at day 0, 7, 10, 17, 21, 24 (including post-infusion samples at end of 2h infusion for RMD recipients at day 10, 17 and 24), 30, 60, 90, 180, 270 and 365 after ART initiation and every week for the first 8 weeks of the ATI and subsequently biweekly for the last 4 weeks. Blood samples were processed within 4 hours of collection, and serum and plasma samples were stored at −80 °C. Peripheral blood mononuclear cells (PBMCs) were isolated by density gradient centrifugation and cryopreserved in fetal bovine serum with 10% dimethyl sulfoxide (DMSO). Clinical safety assessments included directed physical examinations, vital sign measurement, review of adverse events and concomitant medications at every visit and reported until the end of study (Fig. 1a). The Common Terminology Criteria for Adverse Events (CTCAE) v4.03 grading scale was used to grade adverse events. No safety monitoring committee was involved since the interventional period was relatively short and the study drugs are well-characterized. Safety biochemistry was taken day −28-0, 7, 10, 17, 21, 24 and 365 days after ART initiation. Plasma HIV-1 RNA levels were measured with standardized clinical assays at every visit. CD4+ T cell counts were measured on day −28–−1, baseline (day 0), day 10, 17, 24, 30, 90, 180, 270 and 365. Of the 52 individuals that could participate in the optional ATI, only 20 individuals participated, 29 individuals were not willing to participate due to personal reasons and 3 individuals were willing, but not eligible for participation (Extended Fig. 1). During ATI, plasma HIV-1 RNA levels, CD4+ T-cell counts, and safety assessments were conducted every week for the first 8 weeks and subsequently biweekly. After resumption of ART, we monitored plasma HIV-1 RNA levels every fourth week until levels were undetectable (<20 copies/mL) on 2 consecutive measurements. We acknowledge the lack of Data and Safety Monitoring Board, but the study design allowed designated investigators at each site with access to all data. All safety data and medical notes were monitored by external monitors from the Danish Good Clinical Practice Units.

HIV-1-infected cells using the FISH-flow assay

Multiparametric characterization of the transcriptional and/or translational activity of HIV-1-infected cells was done using a Human PrimeFlow RNA Assay Kit (AH diagnostics A/S) according to a well-established HIV-1 RNA fluorescence in situ hybridization-flow cytometry assay (FISH-flow assay) protocol[38]. We used samples from the interventional

period in a subset of participants at 5 or 8 time points: baseline (day 0), day 10, 17, 24, (+ three post-infusion timepoints for RMD recipients) and 30 after ART initiation. To ensure the collection of 3×10^6 cells at the final step of acquisition on the flow cytometer, we began with at least 3×10^7 frozen PBMCs of the individuals at each time point. Samples obtained at different time points that derived from the same individual were always assayed simultaneously using identical reagent master mixes in order to minimize any potential batch effect. Only singlet, live cells were included in the data analyses. Samples were gated on CD3+CD8− T cells due to downregulation of CD4: Lymphocytes > single cells (forward scatter) > single cells (side scatter) > live CD3+ cells > CD8− cells > HIV-1 RNA+ and Gag p24+ (Supplementary Fig. S4). Transcriptionally active HIV-1-infected cells were identified as HIV-1 mRNA+. HIV-1-infected cells both transcriptionally and translationally active were identified as HIV-1 mRNA+ and Gag p24+. Translationally active HIV-1-infected cells were identified as Gag p24+. Due to a faulty mRNA probe in the 2nd batch of FISH-flow analyses, mRNA data was only available for half of the study population analyzed by FISH-flow assay (Fig. 1b). Of note, the analyses were not done on specific selected individuals, but on all individuals for whom we had sufficient quantities of cryopreserved PBMCs (with a viability >70% after thawing and resting) at multiple study time points during the first 30 days after starting ART. The FISH-flow assay was validated based on the correlations between CD3+CD8− T cells expressing either mRNA, p24 or both and plasma HIV-1 RNA[67,68], CD4+ T cell count[67,68] and the CD4/CD8 ratio[68]. Memory subsets within the CD3+CD8− T cells were defined based on CD27 and CD45RA expression: Central memory T cells (T_{CM}): CD27+CD45RA-, naïve T cells (T_N): CD27+CD45RA+, effector memory T cells (T_{EM}): CD27-CD45RA-, and terminally differentiated T cells (T_{TD}). T follicular helper cells (T_{FH}) were defined based on CXCR5 and PD-1 expression. The immunofluorescent monoclonal antibodies BUV395-CD4 (Clone: SK3), BUV496-CD8 (Clone: RPA-T8), BUV737-CD3 (Clone: UCHT1), BV605-CD27 (Clone: L128), BV786-Ki-67 (Clone: B56) and BB515-CD185 (CXCR5) (Clone: RF8B2) were purchased from BD Pharmingen. The Human TruStain FcX, BV711-CD45RA (Clone: HI100), PE-Cy7-PD-1 (Clone: EH12.2H7), and Zombie Violet were purchased from BioLegend. For labeling HIV-1 Gag p24 protein, cells were intracellularly stained with PE-P24 (Clone: KC57-RD1, Beckman Coulter). All the samples were analyzed on a LSRFortessa™ X-20 Flow Cytometer (BD Biosciences) and flow cytometry data were analyzed using FlowJo software, version 10.6.0 (Tree Star).

HIV-1-speficifc CD8+ T cell immunity using the AIM assay.

We assessed HIV-1-specific CD8+ T cell immunity using the activation-induced marker (AIM) assay by flow cytometry at baseline (day 0), 90 and 365 days after ART initiation. Cryopreserved PBMCs were thawed, washed and rested at 37°C for 3 hours. Cells were then plated into wells of a 96-well plate, at a total of $1x10^6$ cells per well. For each assay, 5 conditions were used: no exogenous stimulation with DMSO as negative control, four HIV-1 antigen stimulations and staphylococcal enteroxin B (SEB, 1 μg/ml) as positive control. The antigen stimulations were overlapping peptide pools corresponding to HIV-Gag (JPT, PM-HIV-Gag), HIV-ENV (JPT, PM-HIV-ENV), HIV-NEF (JPT, PM-HIV-Nef) and HIV-POL (JPT, PM-HIV-Pol) used at a final concentration of 2 μg/mL of total peptide. Following 20 hours incubation at 37°C, cells were washed with PBS and stained for viability with Near IR Dead Live Dead for 20 minutes. Cells were then incubated with

Human TruStain FcX (BioLegend) in PBS 2% FBS for 10 minutes and stained 30 minutes with surface markers antibodies: CD3 (PerCP/Cy5.5 anti-human CD3, SK7, BioLegend), CD4 (BV650 anti-human CD4, RPA-T4, BioLegend), CD8 (BV605 anti-human CD8a, RPA-T8, BioLegend), 4-1BB (PE anti-human CD137, BioLegend) CD69 (APC anti-human CD69, FN50, BioLegend) and PD-L1 (BV421 anti-human CD274, B7-H1, BioLegend). Cells were washed twice and acquired on a on MACSQuant16. Data were analyzed using FlowJo 10.6.0. The frequency of antigen-specific cells (AIM+ cells) was determined by subtracting the frequency of the non-stimulation condition from the antigen stimulated conditions. AIM+ cells were considered as the addition of the frequency of cells that were either CD69+PD-L1+4-1BB+, CD69+PD-L1+, CD69+4-1BB+ or PD-L1+4-1BB+. Total HIV-specific AIM+ cells was calculated as summation of each of the 4 populations for the four antigen-stimulations. In this paper, we report the HIV-1 Gag-specific CD8+ T cell immunity only, while a detailed description of the HIV-1-specific T cell immunity is reported in an unpublished manuscript by Rosas-Umbert M. et al.

Intact HIV-1 proviruses by duplexed droplet digital PCR (3dPCR)

We applied a 3dPCR assay adapted from the IPDA protocol, which is specific for HIV-1 subtype B[40]. Duplexing increases the selectivity of molecular assays to identify genomically-intact proviruses, particularly when primer/probe sets are placed in locations that are highly predictive of proviral integrity. The IPDA achieves this by targeting the Ψ and RRE which are frequently deleted or mutated in defective proviruses[40]. As a substantial proportion of individuals harbored non-B infections, we performed an IPDA-like 3dPCR assay that leverages these principles, using autologous primers/probes where necessary to accommodate HIV polymorphism. The two HIV regions targeted by the 3dPCR assay were the Ψ region featured in the published IPDA[40], and a region within the RRE in *envelope,* located slightly downstream of the original IPDA *env* primer/probe set, that has previously been used as a secondary ("backup") location for this assay[41]. The published primer/probe sequences for these regions are: HIV-1 Ψ Forward Primer- CAGGACTCGGCTTGCTGAAG, HIV-1 Ψ Probe- FAM-TTTTGGCGTACTCACCAGT-MGBNFQ, HIV-1 Ψ Reverse Primer- GCACCCATCTCTCTCCTTCTAGC, HIV-1 Secondary *env* Forward Primer- ACTATGGGCGCAGCGTC, HIV-1 Secondary *env* Probe VIC- CTGGCCTGTACCGTCAG- MGBNFQ, and HIV-1 Secondary *env* Reverse Primer- CCCCAGACTGTGAGTTGCA (Supplementary Table S2). While the 3dPCR assay has not been formally validated to the same extent as the IPDA for genomic integrity prediction, the two assays feature identical 5' primer/probe locations in Ψ, and partially overlapping 3' primer/probe locations in *env*, where the latter are situated within a region that is highly predictive of intact proviruses, at least in HIV-1 subtype B[40].

To assess whether the published primers/probes were appropriate for each participant or whether autologous oligonucleotide design would be required, we sequenced the Ψ and *env* assay regions from pre-ART plasma HIV-1 RNA samples for all participants for whom samples were available for 3dPCR. Plasma HIV-1 RNA was sequenced so that any autologous primers/probes would capture intact HIV sequences to guide oligonucleotide design. Briefly, single-template amplification and sequencing was performed for *env* with gene-specific primers as described below. For Ψ, RNA

extraction and cDNA synthesis was performed as for *env* with the gene-specific primer 2crx: 5' – TAACCCTGCGGGATGTGGTATTCC -3'. Bulk nested PCR was conducted with Platinum Taq DNA polymerase High Fidelity (Invitrogen) using the following primers: first round PCR- forward 5' – AAATCTCTAGCAGTGGCGCCCGAACAG -3', reverse out 5' – TAACCCTGCGGGATGTGGTATTCC -3', second round PCR- forward 5' – GCGCCCGAACAGGGACYTGAAARCGAAAG -3', reverse 5' – TATCATCTGCTCCTGTATC -3'. The Ψ samples were sequenced as described for *env*. Supplementary Table S2 reports the participant HIV-1 sequences within these 3dPCR primer/probe regions, along with the sequence of any autologous oligonucleotides that were designed to accommodate HIV-1 polymorphism in 3dPCR. For participants with polymorphism at critical residue(s), we designed custom primers/probes that matched their autologous sequence exactly. Polymorphisms at critical residues observed at a within-host frequency of less than 10% were not incorporated into autologous primer/probe design.

Briefly, CD4+ T-lymphocytes were isolated from PBMCs by negative selection (CD4+ T cell isolation kit, Miltenyi) and genomic DNA was extracted (DNeasy Blood and Tissue kit, Qiagen). To quantify proviruses, DNA extracts were assayed with either the published or autologous HIV-1 primer/probe sets, as described in Supplementary Table S2. In parallel, all DNA extracts were also assayed in a separate duplexed ddPCR reaction targeting the human *RPP30* gene[41], using the following primers and probes: *RPP30* Forward Primer- GATTTGGACCTGCGAGCG, *RPP30* Probe- VIC-CTGACCTGAAGGCTCT-MBBNFQ, *RPP30* Reverse Primer- GCGGCTGTCTCCACAAGT, RPP30-Shear Forward Primer- CCATTTGCTGCTCCTTGGG, *RPP30*- Shear Probe- FAM-AAGGAGCAAGGTTCTATTGTAG-MGBNFQ, *RPP30* Shear Reverse Primer-CATGCAAAGGAGGAAGCCG. HIV-1 and human *RPP30* copies were then normalized to the quantity of input DNA to estimate Intact HIV-1 copies/10^6 CD4+ T-cells. Each ddPCR reaction contained genomic DNA, ddPCR Supermix for Probes (no dUTPs, BioRad), primers (final concentration 900nM, Integrated DNA Technologies), probes (final concentration 250nM, ThermoFisher Scientific), *XhoI* restriction enzyme and nuclease free water. Droplets were prepared using a QX200 Droplet Generator (BioRad) and cycled at 95°C for 10 min; 45 cycles of (94°C for 30 sec, 59°C for 1 min) and 98°C for 10 min, using a ramp rate of 2°C to improve droplet separation. Droplets were analyzed on a QX200 Droplet Reader (BioRad) using QuantaSoft software (BioRad, version 1.7.4), where replicate wells were merged prior to analysis. Intact HIV-1 copies (Ψ and *env* double-positive droplets) were corrected for DNA shearing based on the frequency of *RPP30* and *RPP30*-Shear double-positive droplets. The median (IQR) DNA shearing index (DSI), measuring the proportion of sheared DNA in a sample, was 0.34 (0.32-0.39), comparable to that reported in the original development of the IPDA. Using the 3dPCR assay, we measured frequencies of double-positive HIV-1 proviruses (intact), 5' and 3' defective HIV-1 proviruses at baseline (day 0), day 180 and 365 after ART initiation. At baseline, the level of intact proviruses correlated with frequency of induced p24+ CD4+ T cells, plasma HIV-1 RNA level and CD4+ T cell count (Supplementary Fig. S1c-e).

Intact proviruses were also quantified by the IPDA[40] for 23 participants for whom sufficient sample was available at either day 180 (n=4) or day 365 (n=19) time points. Reactions were prepared and analysis was performed as described above

for 3dPCR. Primers and probes targeting HIV-1 were: HIV-1 Ψ Forward Primer-CAGGACTCGGCTTGCTGAAG, HIV-1 Ψ Probe- FAM- TTTTGGCGTACTCACCAGT-MGBNFQ, HIV-1 Ψ Reverse Primer- GCACCCATCTCTCTCCTTCTAGC; HIV-1 env Forward Primer-AGTGGTGCAGAGAGAAAAAAGAGC, HIV-1 env Probe-VICCCTTGGGTTCTTGGGA-

MGBNFQ,anti-Hypermutant env Probe-CCTTAGGTTCTTAGGAGC- MGBNFQ, HIV-1 env Reverse Primer-GTCTGGCCTGTACCGTCAGC. Supplementary Table S3 reports the sequence of these participants in the IPDA Ψ and *env* regions.

The level of intact proviruses measured by IPDA and 3dPCR correlated strongly in individuals with HIV-1 subtype B whose reservoirs could be measured using the former (6 participants could not be measured by IPDA dure to polymorphisms that caused signal failure). The frequency of intact proviruses as measured by 3dPCR was also comparable between individuals with HIV-1 B versus non-B subtypes. This together suggests that 3dPCR provides a reasonable estimate of intact HIV-1 reservoir size, though it is possible that the assay's positive predictive value for intact proviruses may, like the IPDA, vary between individuals[69].

HIV-antigen producing cells using the VIP-SPOT assay

We measured HIV-antigen producing cells using the viral protein spot (VIP-SPOT) assay[39] at baseline (day 0) and 365 days after ART initiation. The measures of HIV-antigen producing cells per 10^6 CD4+ T cells correlated with baseline plasma HIV-1 RNA and intact HIV-1 proviruses (Supplementary Fig. S1b-c). Briefly, CD4+ T cells were isolated from $20x10^6$ cryopreserved PBMCs by negative immunomagnetic separation using the autoMACS® Pro Separator (CD4+ T Cell Isolation Kit, Milteny) according to manufacturer's instructions, and counted using the automated NucleoCounter NC-3000 (Chemometec, Denmark). Median viability of isolated CD4+ from was 94% (range 72–99%). Cell suspensions containing up to 2 $x10^6$ /mL of purified CD4+ T cells were prepared in culture media and distributed at 150 µl per well, so $3x10^5$ cells per well were seeded in the pre-coated ELISpot plates. In all VIP-SPOT assays, CD4+ T cells from individuals without HIV-1 were included as negative control using PBMCs isolated from the buffy coats. The buffy coats were purchased from the Catalan Banc de Sang i Teixits (http://www.bancsang.net/en/index.html; Barcelona, Spain). Likewise, all plates included two positive control wells containing J-Lat cells (clone 8.4) at an approximate ratio of 10^2 cells/well, in culture media supplemented with 20nM PMA and 0.5 µg/ml Ionomycin (P1585 and I3909, Sigma-Aldrich). The VIP-spot assay was analyzed accordance with the published method[39]. .The frequency of HIV-antigen producing cells was determined based on the total number of spots detected for each sample and the amount of CD4+ T cells cultured.

3BNC117 sensitivity testing by either pheno- or geno-typic assays

Post-hoc 3BNC117 sensitivity was performed post-enrollment for participants receiving 3BNC117 using the Labcorp-Monogram Biosciences PhenoSense ® HIV Monoclonal Antibody Assay on plasma HIV-1 RNA viruses. 3BNC117 sensitivity was not a pre-

specified inclusion criterion. Sensitivity was defined in this study as a concentration of 3BNC117 required to inhibit viral replication by 90% (IC90) <1.5 μg/mL and the maximum percent inhibition (MPI) observed at the highest 3BNC117 concentration tested >98%. If the Labcorp-Monogram assay did not yield a result due to lack of insufficient amplification or infectivity, *env* sequences obtained by single genome amplification of plasma RNA viruses from baseline were analyzed using a genotypic prediction algorithm with a pre-defined threshold of 10% of resistant sequences.

Plasma envelope sequencing—To sequence single viral envelope, RNA was extracted from baseline plasma virus using QIAamp Viral RNA Mini Kit (Qiagen) and cDNA synthesized with an envelope specific primer (OFM19: 5'–GCACTCAAGGCAAGCTTTATTGAGGCTTA – 3′) using Superscript III Reverse Transcriptase (Invitrogen™) and RNAseOUT (Invitrogen™) with the following thermal cycling conditions; 50°C for 1hr, 55°C for 1hr and 70°C for 15 minutes. The cDNA was diluted for nested PCR to obtain single genome amplification (<30% of wells containing envelope). The PCR reactions were performed in 10μL using Platinum Taq DNA polymerase High Fidelity (Invitrogen™). In the first PCR the following primers were used; OFM19: 5'– GCACTCAAGGCAAGCTTTATTGAGGCTTA – 3' and VIF1: 5'– GGGTTTATTACAGGGACAGCAGAG – 3' and for the second PCR the ENV A: 5'–GGCTTAGGCATCTCCTATGGCAGGAAGAA – 3' and ENV N: 5'–CTGCCAATCAGGGAAGTAGCCTTGTGT – 3' was used. Envelope positive wells were determined by using E-gel™ (Invitrogen) and collected on a 384 well plate. The concentration was measured for representative wells and all samples diluted to approximately 20ng/μL. For library preparation the samples were first subjected to tagmentation as follows; 1μL DNA 1.25μL Tagment DNA Buffer and 0.25μL TDE1 Tagment DNA enzyme (Illumina). Then unique i5/i7 barcoded primers were ligated to the tagmented DNA with use of KAPA HIFI Hotstart ReadyMix (Roche). The barcoded amplicons were first pooled into eight Eppendorf tubes and purified with AMPure XP Beads (Beckman Coulter) and then pooled together to one library. The library was paired-end sequenced on a MiniSeq (Illumina) with MiniSeq Mid Output kit (300-cycles).

HIV-1 sequence assembly and annotation—HIV-1 sequence assembly was performed by The Rockefeller University pipeline (Defective and Intact HIV Genome Assembler), which is capable of reconstructing thousands of HIV genomes within hours via the assembly of raw sequencing reads into annotated HIV genomes. The steps executed by the pipeline were as follows. First, we removed PCR amplification and performed error correction using clumpify.sh from BBtools package v38.72 (https://sourceforge.net/projects/bbmap/). A quality control check was performed with Trim Galore package v0.6.4 (https://github.com/FelixKrueger/TrimGalore) to trim Illumina adapters and low-quality bases. We also used bbduk.sh from BBtools package to remove possible contaminant reads using HIV genome sequences, obtained from Los Alamos HIV database, as a positive control. Paired-overlapping reads were exported into a single read by BBMerge. We used a k-mer–based assembler, SPAdes v3.13.1, to reconstruct the HIV-1 sequences. The longest assembled contig was aligned via BLAST to with HXB2, to set it the correct orientation. Finally, the HIV genome sequence was annotated by aligning against HXB2 using BLAST. Sequences

with double peaks, i.e., regions indicating the presence of two or more viruses in the sample (cutoff consensus identity for any residue <70%), or samples with a limited number of reads (empty wells ≤500 sequencing reads) were omitted from downstream analyses. In the end, sequences were classified as intact or defective.

Sequence-based assessment of 3BNC117-sensitivity—Analysis of HIV-1 *env* mutations that have been described to correlate with resistance to 3BNC117 was performed in the obtained sequences by a post-hoc model based on sequencing and neutralization data to predict virus sensitivity. Based on published data, the following amino acid rules (using HXB2 numbering) were used to determine 3BNC117-sensitive strains.15 N or D at 279, not K or D at 280, R at 456, D at 457, G at 458, G at 459, no PNGS at 279 (not N279 and S or T at 281).

All viral sequences have been deposited in GenBank with accession numbers ON542594 to ON542710.

Human leukocyte antigen class I typing

Human leukocyte antigen (HLA) class I (HLA-A, -B, -C) alleles were genotyped at the American Safety and Health Institute-accredited laboratory HistoGenetics (Ossining, New York, US) using sequence-based typing.

Asanté Recency Testing

Recency testing was performed on plasma obtained at baseline using the Asanté HIV-1 Rapid Recency Assay (Sedia Biosciences Corporation, Beaverton, Oregon, USA) according to the manufacturer's protocol[70].

12-week Analytical Treatment Interruption

Enrollment into the 12-week ATI was optional and conditioned by the following criteria on individual level:

1. Undetectable plasma HIV-1 RNA levels <50 copies/mL during the last 6 months (one 'viral blip' >50 copies/mL was acceptable)
2. Latest CD4+ T cell count >500 cells/mm^3

The following criteria were used to restart ART:

1. Two consecutive plasma HIV-1 RNA measurements >5,000 copies/mL
2. CD4+ T cell count <350 cells/mm^3
3. Participant request
4. If ART interruption in the opinion of the Sponsor or Investigator contained an unacceptable risk to the participant

OUTCOMES

The primary endpoints were 1) viral decay kinetics after ART initiation using plasma HIV-1 levels; and 2) changes in reservoir size measured by double-positive HIV-1 proviruses and HIV-Ag producing cells per 10^6 unfractionated CD4+ T cells. Secondary endpoints were 1) safety including CD4+ T cell counts; 2) changes in the transcriptionally and/or translationally active HIV-1-infected cells during the first 30 days of ART using FISH-flow assay 3) effects on HIV-1 Gag-specific T-cell immunity using the AIM assay; 4) time to loss of virologic control during ATI. We defined loss of virologic control as two consecutive plasma HIV-1 RNA measurements of ≥5,000 copies/mL. If CD4+ T-cell counts decreased to <350 cells/mm^3, ART was also resumed[71]. 5) post-hoc baseline (day 0) sensitivity to 3BNC117 and recency testing.

STATISTICAL METHODS

At the time of protocol development, there was no validated PCR assay for estimating the size of the intact proviral reservoir, so the sample size was based on anticipated changes in total HIV-1 DNA. The anticipated average individual change in total HIV-1 DNA was approximately −0.85 per 10^6 CD4+ T cells on the log10 scale with corresponding standard deviation (SD) 0.35 from baseline (time of ART initiation) to 365 days after ART initiation, when not receiving 3BNC117 or RMD[72]. One of the primary endpoints was change in total HIV-1 DNA from baseline to 365 days after ART initiation in the ART+3BNC117+RMD group compared to the ART only group. The ART+3BNC117 and ART+RMD groups were used to compare secondary endpoints in terms of the specific effects of each of the interventions alone, but the trial was powered according to the decline in total HIV-1 DNA in the ART only and ART+3BNC117+RMD groups: δART and $\delta ART+3BNC117+RMD$. Based on a two sample mean comparison under the null-hypothesis $H0$: $\delta ART = \delta ART+3BNC117+RMD$ and expected values of−0.85 and −1.35, respectively, and an SD of 0.35, a power of 90% is achieved with enrolment of 12 participants in each arm at a 5% significance level. To accommodate for dropouts, we aimed for 15 participants in each arm. We considered a two-sided α value of less than 0.05 significant. We later used the d3PCR assay based on the IPDA protocol and used this as our primary reservoir measurement as we believe that the 3dPCR assay is superior to total HIV-1 DNA in terms of estimating the intact HIV-1 reservoir. Protocol amendments did not affect the analysis plan besides the reservoir size analyzes described above. The analyses performed on primary and secondary endpoints were prespecified in the protocol, and no exploratory analyses were done, hence no corrections for multiple comparisons were made.

We used multiple imputation to impute missing values in plasma HIV-1 RNA. Such missing values could occur due to a measurement not being conducted or being below the limit of quantification (<20 copies/ml). After ln-transformation of the plasma HIV-1 RNA, we used linear regression in the imputation model for absent measurements and interval regression for measurements below the quantification limit. As predictors in the regression models, we used the previous and the subsequent measurement. Using interval regression together with multiple imputation is a standard approach for handling interval censored data, including situations with censoring due to a quantification limit. The method also handles missing

values by interval censoring[73]. In brief, based on observed and (interval) censored values the method estimates how the mean of ln-transformed plasma HIV-1 RNA depends on a linear function of covariates, assuming that the outcomes follow a normal distribution with an unknown, but constant variance. This model is completely similar to ordinary linear regression, although observations may now be intervals instead of specific values. Once the mean function and variance were estimated, imputation values for the missing data were generated from a truncated normal distribution for the interval-censored observations using standard random number generation techniques. To achieve good asymptotic properties of estimates we imputed 100 datasets. The analysis of multiple imputed datasets was done via Rubin's formula, which states that analyses of each imputed dataset may be validly joined into a single combined estimate[74,75]. Mixed-effects linear regression models with a random effect for individual participants were used to analyze decay rates between groups. Paired two-tailed Wilcoxon tests and two-tailed Mann-Whitney tests were used to analyze nonparametric outcomes within- and between groups, respectively. When more than two groups were using nonparametric statistics, the Kruskal–Wallis test was used. Paired and unpaired t tests were used to analyze parametric outcomes within- and between groups, respectively. Fisher's exact test was used to analyze contingency tables. Data are presented as either median (IQR), median (range), or mean±SD as indicated in each respective figure legend. The Kaplan-Meier estimator was used to assess the magnitude of the difference between the survival curves, and the log-rank test was used to compare time to loss of virologic control during ATI between groups. For correlations, Spearman's correlation coefficient was used. We used the full analysis set, comprising all individuals receiving at least one dose of active treatment with assessable data, for the efficacy analyses, and all enrolled individuals for the safety analyses. We used Stata version 17.0, and Prism version 7.0 for statistical analyses.

Extended Data

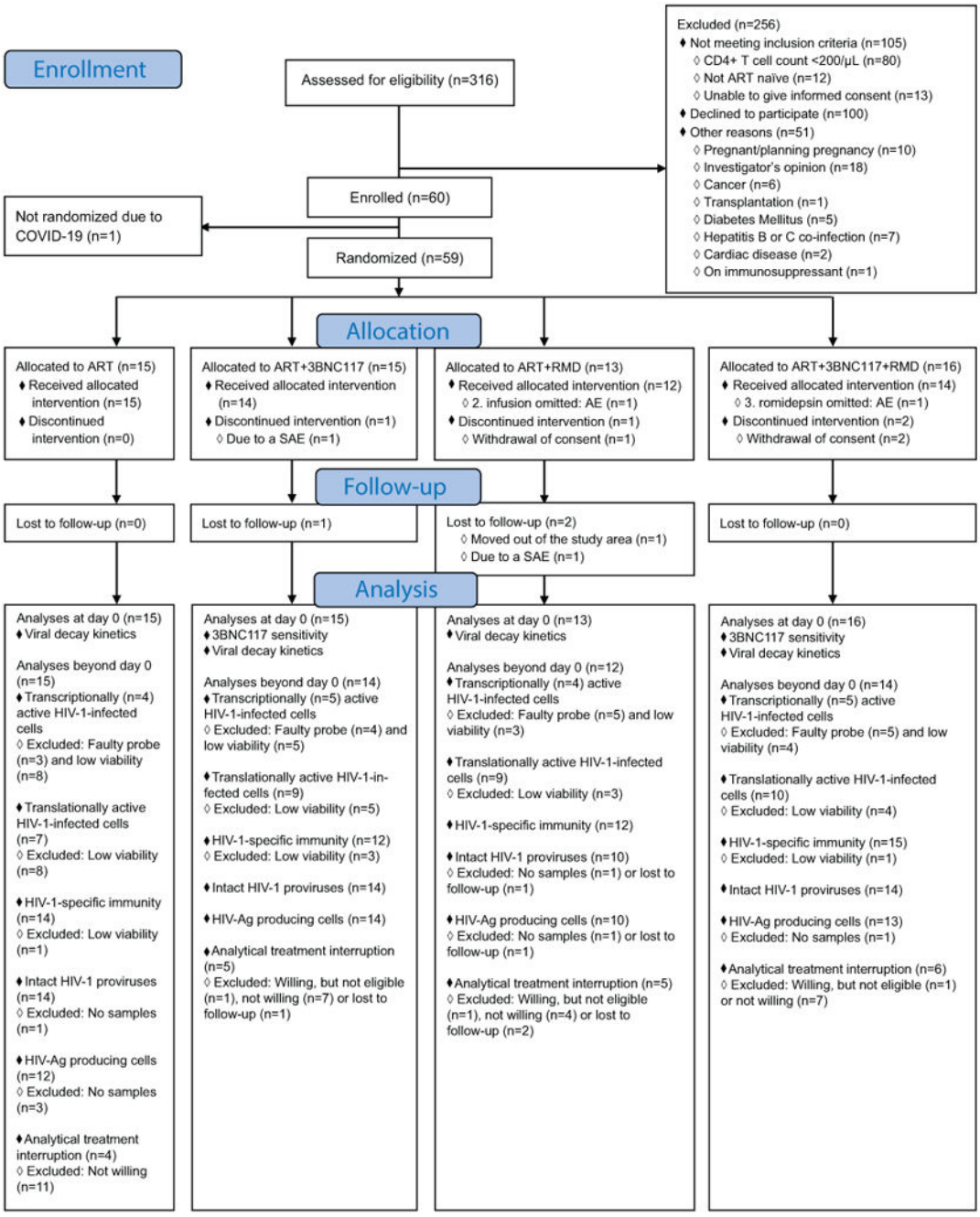

Extended Data Fig. 1. A comprehensive CONSORT Flow Diagram.

AE, adverse event; Ag, antigen; ART, antiretroviral therapy; COVID-19, coronavirus disease 2019; RMD, romidepsin; SAE, serious AE.

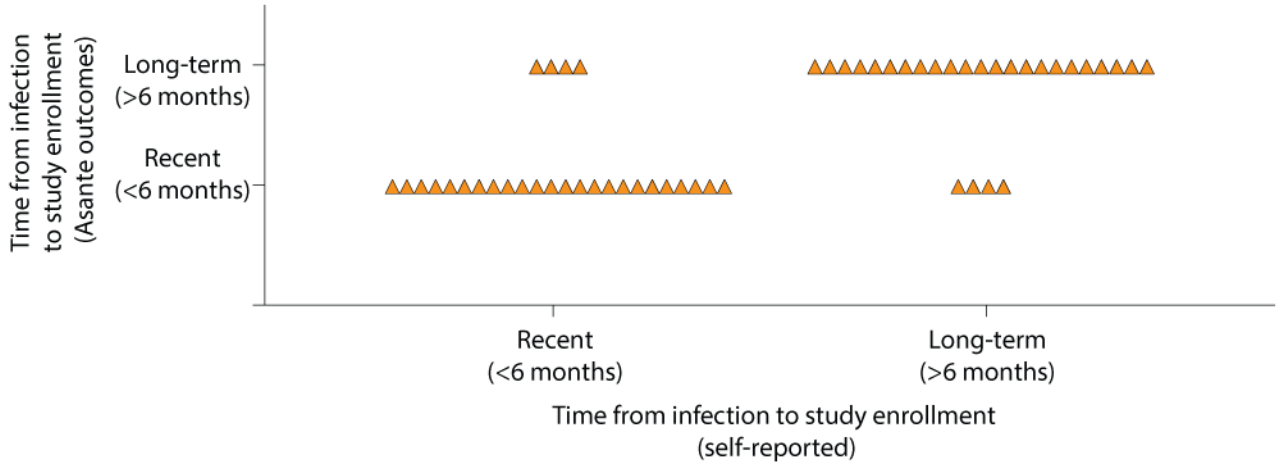

Extended Data Fig. 2. Distribution between self-report time of infection to study enrollment and outcome of the Asanté HIV-1 Rapid Recency Assay (n=54).

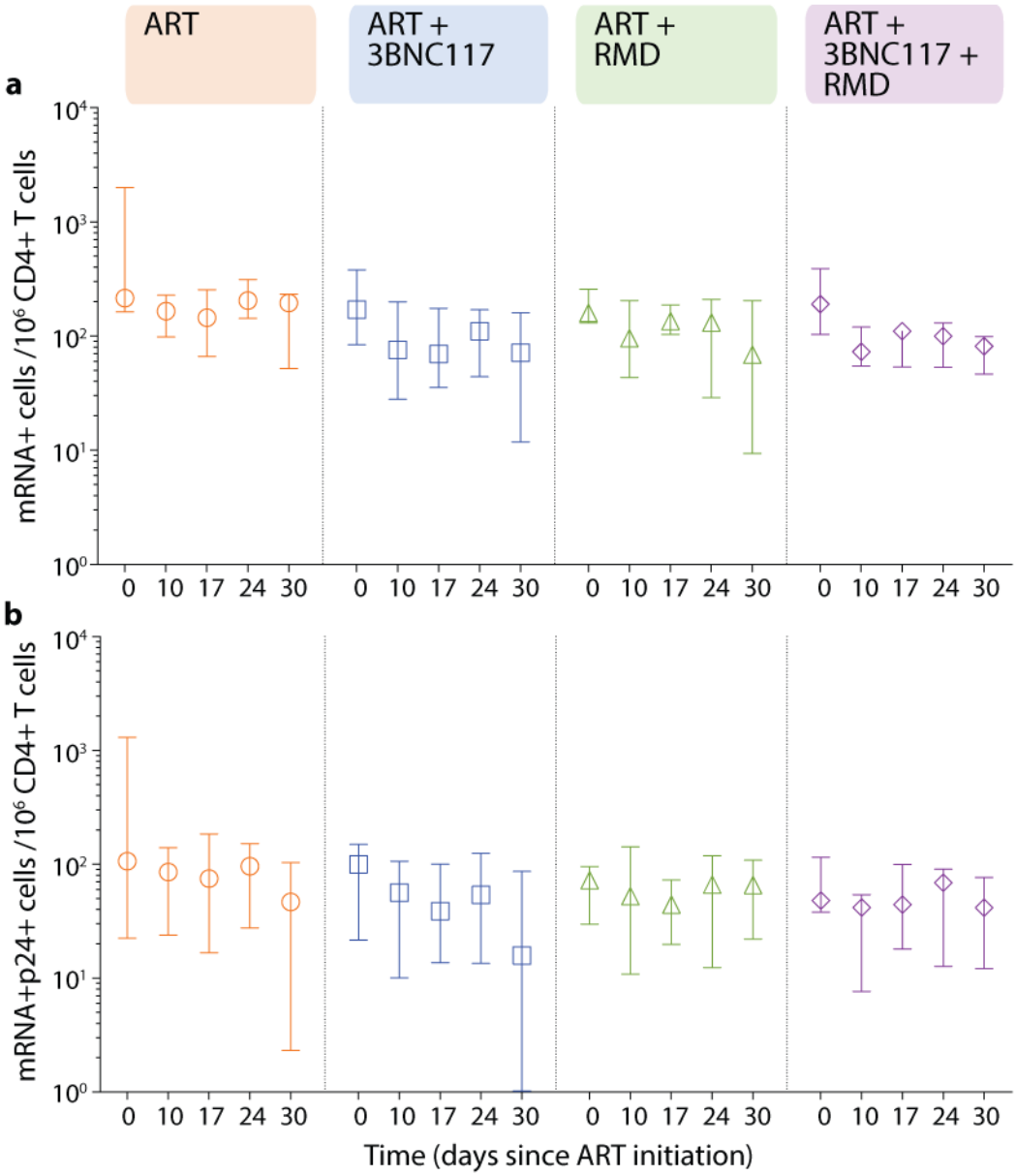

Extended Data Fig. 3. Transcriptionally (mRNA+) and transcriptionally + translationally (mRNA+p24+) active HIV-1-infected cells following ART initiation.

Changes in HIV-1-infected cells during the first 30 days of ART among the four groups shown as median (error bars represents interquartile ranges) number of CD3+CD8− T cells expressing either HIV-1 mRNA (**a**) or HIV-1 mRNA and Gag p24 protein (**b**). ART-control n=4, ART+3BNC117 n=5, ART+RMD n=4, ART+3BNC117+RMD n=5.

ART, antiretroviral therapy; RMD, romidepsin.

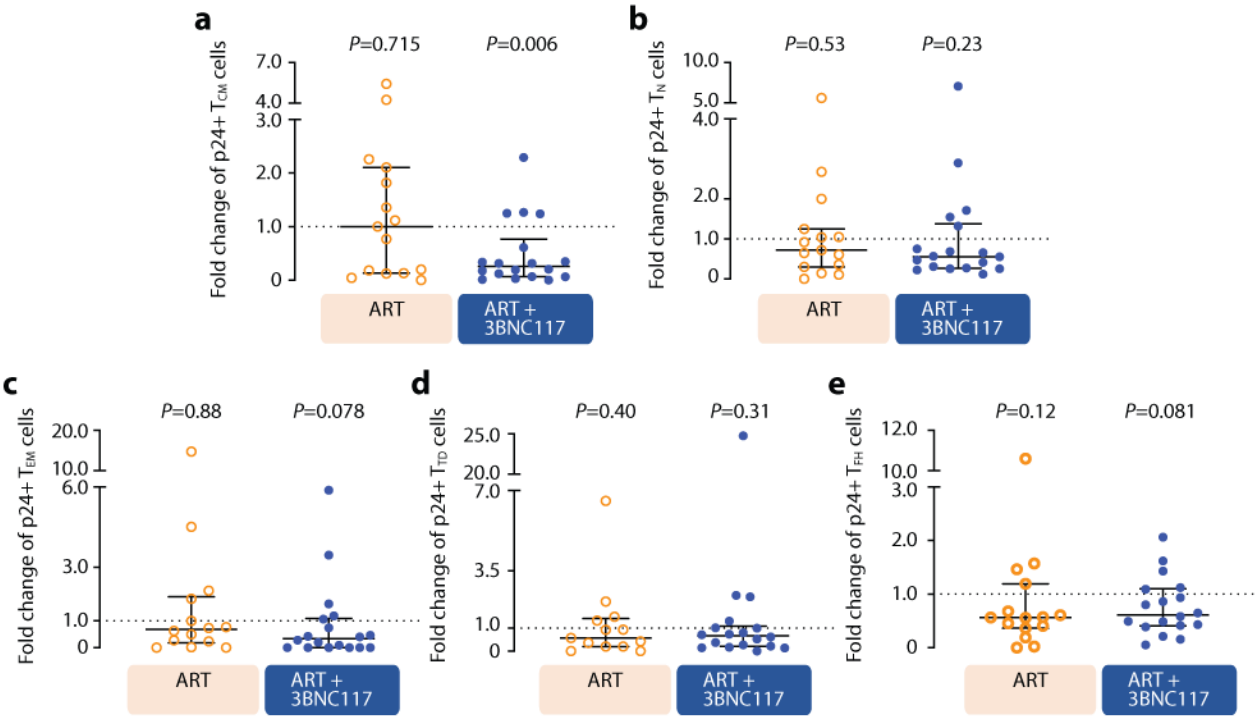

Extended Data Fig. 4. Impact of 3BNC117 on translationally (p24+) active HIV-1-infected CD4+ T cell subsets.

Data are shown as in Fig. 3b-e, where the ART only and ART+RMD groups (who only received ART during the first 10 days) are combined into one group and compared to the two 3BNC117-treated groups. Median (error bars represent interquartile ranges) fold change in CD3+CD8− T cell subsets expressing Gag p24 among the combined ART (n=15) and ART+3BNC117 (n=18) groups. The CD3+CD8− T cells subsets are central memory T cells (T_{CM}) (**a**), naïve T cells (T_N) (**b**), effector memory T cells (T_{EM}) (**c**), terminally differentiated T cells (T_{TD}) (**d**), and T follicular helper cells (T_{FH}) (**e**). *P* values comparing within group was calculated using paired two-tailed Wilcoxon test.

ART, antiretroviral therapy; IQR, interquartile ranges; RMD, romidepsin.

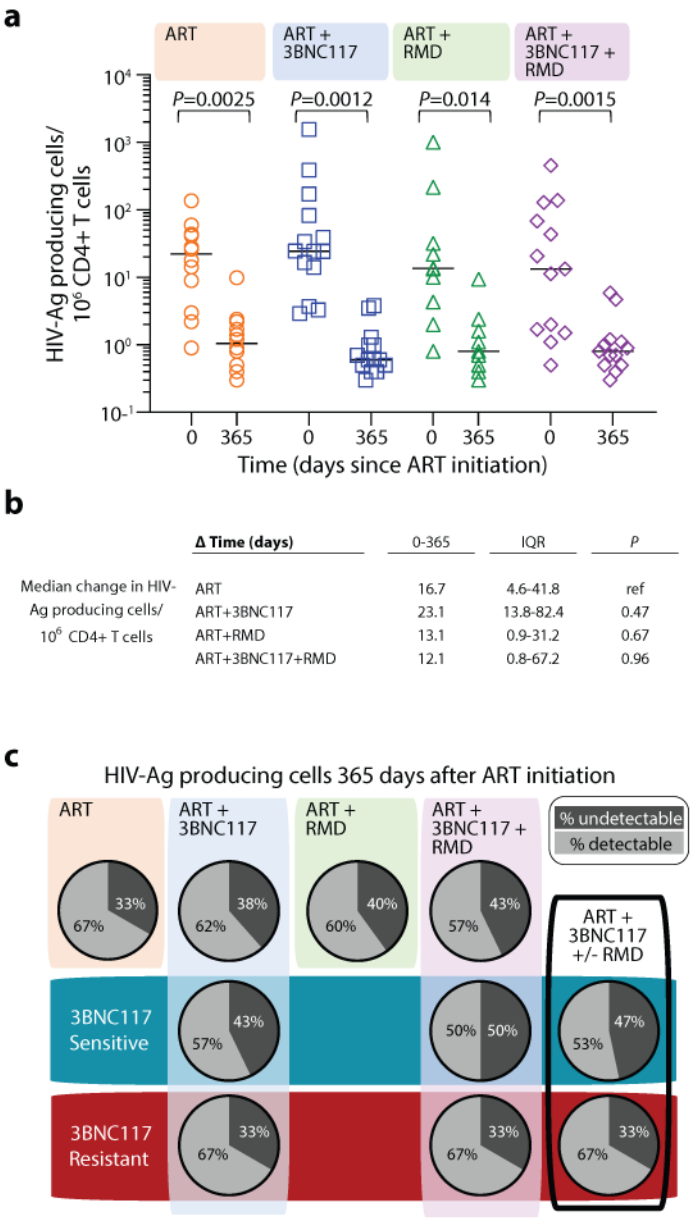

Extended Data Fig. 5. The frequency of HIV-1 antigen-producing cells.

The individual frequency of induced p24+ CD4+ T cells at ART initiation (day 0) and after 365 days of ART (lines at median) (**a**) and median changes in these cells between day 0 and 365 after ART initiation (**b**) among individuals in the four groups. *P* values comparing within group and between groups were calculated using paired two-tailed Wilcoxon test and two-tailed Mann-Whitney test, respectively. Pie charts showing the status of HIV-1 antigen-producing cells after 365 days of ART per group (column and upper row) and categorized according to pre-ART plasma virus sensitivity (middle row; blue shaded area) or resistance (bottom row; red shaded area) to 3BNC117 (**c**). A compiled group ART+3BNC117+/−RMD is shown is the last column. ART-control n=12, ART+3BNC117 n=14, ART+RMD n=10, ART+3BNC117+RMD n=13.

Ag, antigen; ART, antiretroviral therapy; RMD, romidepsin.

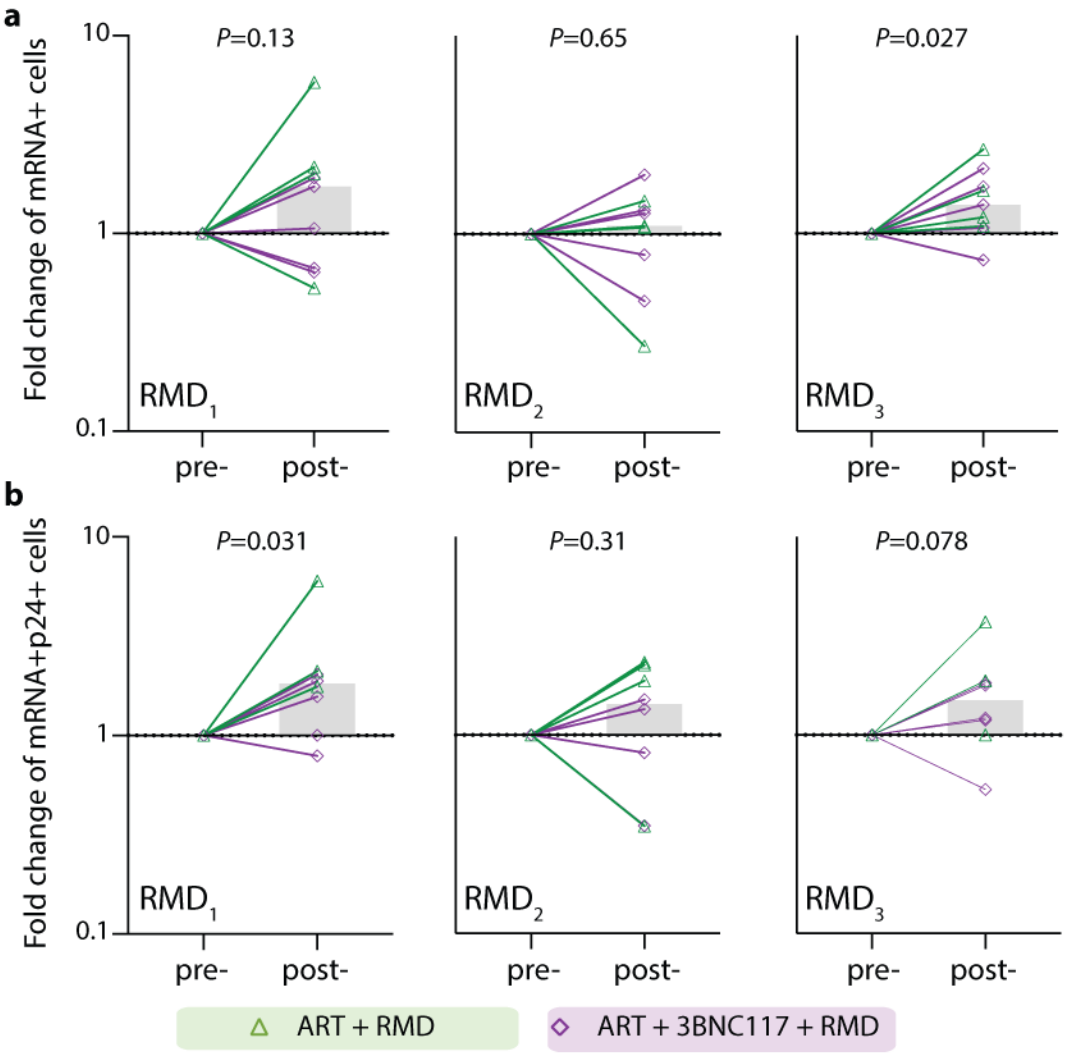

Extended Data Fig. 6. Effect of RMD on transcriptionally (mRNA+) and transcriptionally + translationally (mRNA+p24+) active HIV-1-infected cells.

Data are shown as in Fig. 3f-g. Individual and overall median fold change (column) from pre- to post-RMD infusions in groups ART+RMD (n=8) and ART+3BNC117+RMD (n=10) on CD3+CD8− T cells expressing HIV-1 mRNA (**a**) or mRNA and Gag p24 (**b**). *P* values comparing within group was calculated using paired two-tailed Wilcoxon test. Due to a faulty mRNA probe in the 2nd batch of fluorescence in situ hybridization-flow cytometry analyses, mRNA data was only available for half of the study population.

ART, antiretroviral therapy; RMD, romidepsin.

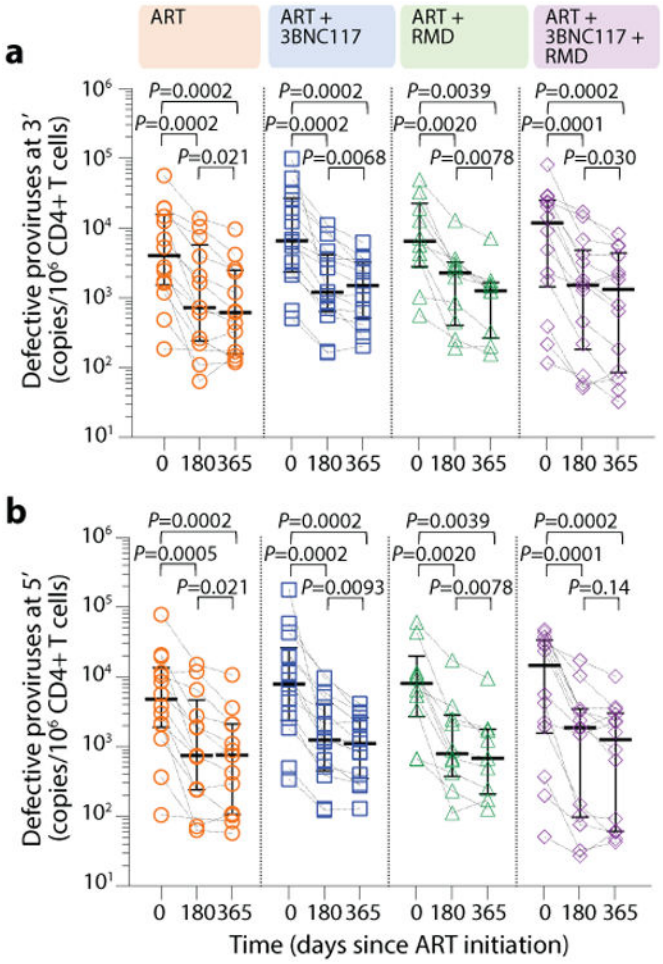

Extended Data Fig. 7. The frequency of defective HIV-1 proviruses.

The frequency of 3' (**a**) and 5' (**b**) defective HIV-1 proviruses at ART initiation and after 180 and 365 days of ART among individuals in the four groups (lines at median, error bars represent interquartile ranges) (**c**). *P* values comparing within group were calculated using paired two-tailed Wilcoxon test. ART only n=14, ART+3BNC117 n=14, ART+RMD n=10, ART+3BNC117+RMD n=14.

ART, antiretroviral therapy; RMD, romidepsin.

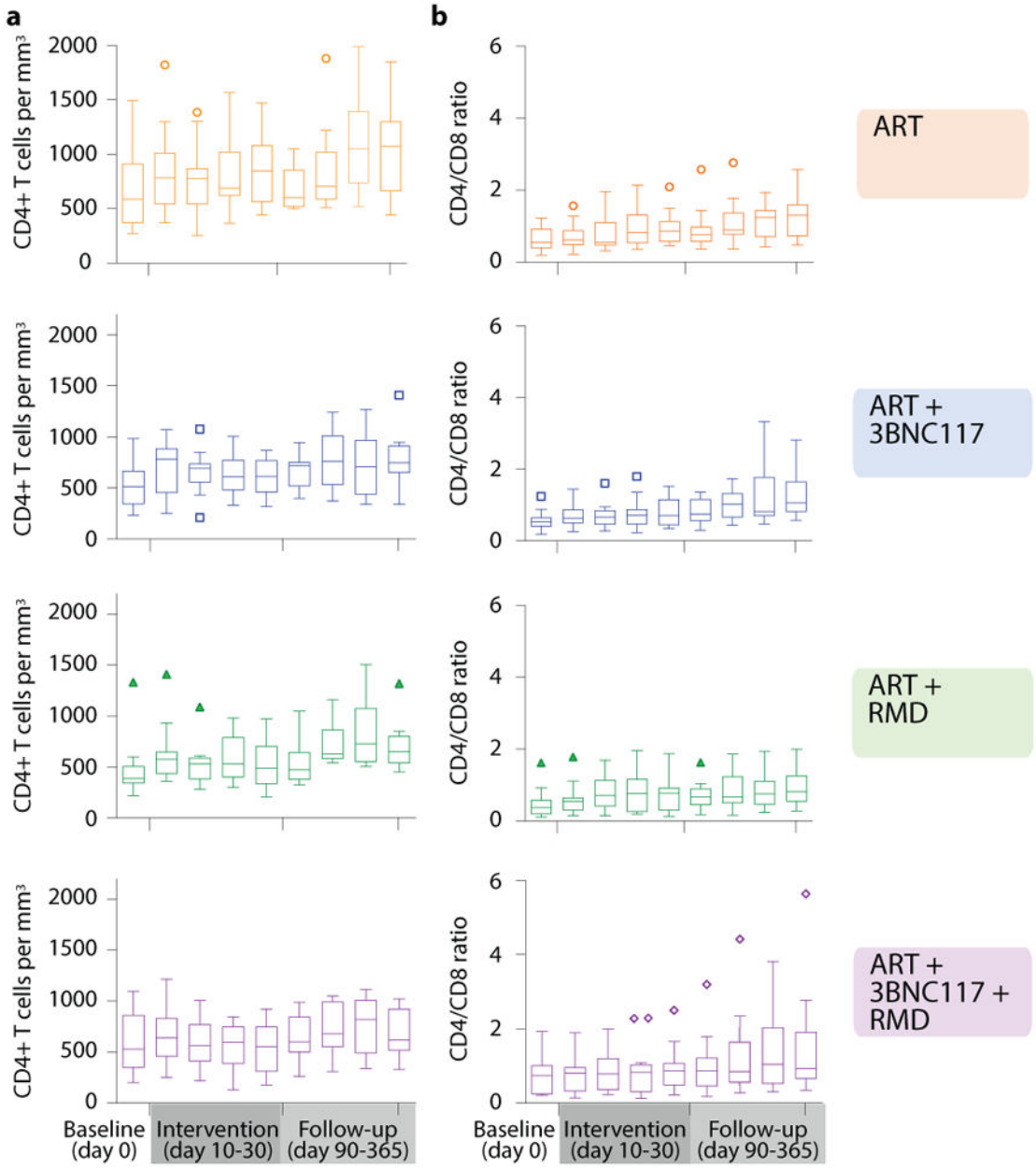

Extended Data Fig. 8. CD4+ T cell count and CD4/CD8 ratio during the study.

Tukey plots depicts the CD4+ T cell count (**a**) and CD4/CD8 ratio (**b**) in the four groups at baseline (day 0), the interventional period (day 10–30) and during follow-up (day 90–365). Lines indicates median, boxes represent interquartile ranges and whiskers drawn within the 1.5 IQR values. ART only n=15, ART+3BNC117 n=15, ART+RMD n=13, ART+3BNC117+RMD n=16.

ART, antiretroviral therapy; IQR, interquartile range; RMD, romidepsin

Extended Table 1.

Individual baseline characteristics for the study population.

		HIV-1 subtype	HLA class I alleles						Plasma HIV-1 RNA (copies/mL)	CD4+ T cells (per mm3)
			A1	A2	B1	B2	C1	C2		
ART-control (n=15)	105	C	02:01:01G	24:02:01G	08:01:01G	15:01:01G	03:03:01G	07:01:01G	290,000	NA
	110	D	01:01:01G	29:02:01G	08:01:01G	44:03:01G	07:01:01G	16:01:01G	88,000	1,440
	120	B	02:03:01	02:03:01	46:01:01	51:01:02	01:02:01G	14:02:01G	15,500	560
	201	C	01:01:01G	23:01:01G	08:01:01G	44:03:01G	04:01:01G	07:01:01G	3,240,000	344
	206	CRF01	01:01:01G	02:01:01G	37:01:01G	44:02:01G	06:02:01G	07:04:01G	78,300	271
	208	CRF other	02:02:01G	02:01:01G	14:02:01G	58:02:01G	06:02:01G	08:02:01G	31,800	NA
	209	B	03:01:01G	30:04:01G	14:02:01G	40:02:01G	02:02:02G	08:02:01G	16,900	948
	305	B	03:01:01G	03:01:01G	07:02:01G	35:01:01G	04:01:01G	07:02:01G	6,415	590
	306	B	11:01:01G	24:02:01G	18:01:01G	35:03:01G	04:01:01G	07:01:01G	4,194	710
	405	F	03:01:01G	03:01:01G	35:03:01G	44:02:01G	04:01:01G	07:04:01G	499,000	765
	407	B	23:01:01G	26:01:01G	49:01:01G	53:01:01G	04:01:01G	07:01:01G	29,200	394
	409	B	01:01:01G	68:02:01G	14:02:01G	57:01:01G	07:01:01G	08:02:01G	39,207	466
	410	B	02:01:01G	24:02:01G	07:02:01G	15:01:01G	03:03:01G	07:02:01G	128,052	886
	702	D	29:02:01G	66:01:01G	18:01:01G	35:01:01G	04:01:01G	05:01:01G	110,000	338
	707	CRF01	02:01:01G	02:01:01G	57:01:01G	57:01:01G	06:02:01G	06:02:01G	820	1,497
ART+3BNC117 (n=15)	106	CRF01	26:01:01G	68:01:02G	07:02:01G	40:01:01G	03:04:01G	07:02:01G	681,000	230

		HIV-1 subtype	HLA class I alleles						Plasma HIV-1 RNA (copies/mL)	CD4+ T cells (per mm3)
			A1	A2	B1	B2	C1	C2		
ART+RMD (n=13)	109	D	11:01:01G	24:02:01G	07:02:01G	39:01:01G	07:02:01G	07:02:01G	22,400	660
	125	B	23:01:01G	26:01:01G	08:01:01G	40:01:01G	03:04:01G	07:01:01G	42,700	290
	126	CRF01	02:06:01G	11:01:01G	15:21:01G	38:02:01G	04:03:01G	07:02:01G	71,900	320
	135	CRF01	24:07:01G	33:03:07	15:01:01G	44:03:02G	04:01:01G	07:01:01G	33,800	NA
	205	B	01:01:01G	02:01:01G	08:01:01G	37:01:01G	06:02:01G	07:01:01G	413,000	984
	210	B	01:01:01G	24:02:01G	08:01:01G	39:06:02G	07:02:01G	07:01:01G	100,000	700
	211	B	11:01:01G	11:01:01G	18:01:01G	51:01:01G	07:01:01G	15:13:01	65,700	414
	302	CRF01	01:01:01G	03:01:01G	14:02:01G	37:01:01G	06:02:01G	08:02:01G	37,726	760
	401	B	02:01:01G	30:02:01G	07:05:01G	44:02:01G	02:02:02G	15:05:01G	33,700	661
	404	A	30:01:01G	68:01:01G	50:01:01G	51:01:01G	15:02:01G	16:01:01G	16,200	457
	412	B	02:01:01G	23:01:01G	35:01:01G	49:01:01G	04:01:01G	07:01:01G	4,190,000	525
	701	B	02:01:01G	02:01:01G	15:01:01G	44:02:01G	03:03:01G	05:01:01G	740	506
	703	CRF02	01:01:01G	24:02:01G	07:02:01G	08:01:01G	07:02:01G	07:01:01G	24,000,000	345
	704	CRF01	01:01:01G	24:02:01G	44:02:01G	57:01:01G	05:01:01G	06:02:01G	56,800	631
	104	B	02:01:01G	02:01:01G	15:01:01G	44:05:01G	02:02:02G	03:28	116,000	600
	108	CRF01	11:01:01G	11:01:01G	40:01:01G	51:01:01G	07:02:01G	14:02:01G	21,061	1,333
	115	B	01:01:01G	34:01:01G	15:21:01G	27:02:01G	02:02:02G	04:03:01G	49,400	490

		HIV-1 subtype	HLA class I alleles						Plasma HIV-1 RNA (copies/mL)	CD4+ T cells (per mm3)
			A1	A2	B1	B2	C1	C2		
ART+3BNC117+RMD (n=16)	117	B	02:01:01G	24:02:01G	40:02:01G	56:01:01G	01:02:01G	02:02:02G	44,200	500
	131	C	29:02:01G	74:01:01G	15:03:01G	42:01:01G	02:10:01G	17:01:01G	3,800	220
	202	B	01:01:01G	01:01:01G	07:02:01G	08:01:01G	07:02:01G	07:01:01G	141,000	354
	204	C	03:01:01G	29:02:01G	07:02:01G	37:01:01G	06:02:01G	07:02:01G	437,000	383
	207	B	01:01:01G	03:01:01G	08:01:01G	15:01:01G	07:01:01G	15:05:01G	43,900	NA
	307	CRF01	01:01:01G	33:01:01G	14:02:01G	50:01:01G	06:02:01G	08:02:01G	16,466	340
	403	A	01:01:01G	24:02:01G	08:01:01G	58:01:01G	03:16	07:01:01G	14,600	513
	406	B	01:01:01G	25:01:01G	08:01:01G	18:01:01G	07:01:01G	12:03:01G	968,000	266
	705	CRF01	02:01:01G	03:01:01G	07:02:01G	40:01:01G	03:04:01G	07:02:01G	110,000	346
	708	CRF02	02:05:01G	24:02:01G	35:03:01G	41:01:01G	04:01:01G	17:01:01G	1,900,000	391
	103	B	24:02:01G	26:01:01G	27:05:02G	38:01:01G	02:02:02G	12:03:01G	730	610
	107	CRF01	02:01:01G	25:01:01G	15:01:01G	44:02:01G	03:03:01G	05:03:01G	188,945	470
	112	G	02:01:01G	68:01:02G	15:78:01	44:02:01G	03:04:01G	07:04:01G	23,100	560
	116	C	01:01:01G	02:01:01G	15:01:01G	57:03:01G	03:04:01G	07:01:01G	69,400	380
	130	CRF01	02:01:01G	02:01:01G	15:01:01G	44:02:01G	03:04:01G	07:04:01G	3,710	260
	203	CRF01	01:01:01G	02:01:01G	07:02:01G	08:01:01G	07:02:01G	07:01:01G	1,450,000	313
	212	CRF47	01:01:01G	02:01:01G	44:02:01G	57:01:01G	05:01:01G	06:02:01G	925,000	NA

		HIV-1 subtype	HLA class I alleles						Plasma HIV-1 RNA (copies/mL)	CD4+ T cells (per mm3)
			A1	A2	B1	B2	C1	C2		
	301	B	02:01:01G	02:01:01G	27:05:02G	44:02:01G	01:02:01G	05:01:01G	16,281	800
	303	CRF02	25:01:01G	68:01:02G	18:01:01G	44:02:01G	05:01:01G	07:01:01G	2,274	930
	304	B	02:01:01G	02:01:01G	40:01:01G	51:01:01G	03:04:01G	15:02:01G	317,431	NA
	308	CRF01	02:01:01G	02:01:01G	49:01:01G	55:01:01G	03:03:01G	07:01:01G	4,180,000	NA
	402	B	01:01:01G	23:01:01G	14:02:01G	45:01:01G	06:02:01G	08:02:01G	18,100	950
	408	B	11:02:01G	24:07:01G	07:05:01G	15:02:01G	07:02:01G	08:01:01G	197,934	203
	411	B	01:01:01G	29:02:01G	52:01:01G	57:01:01G	04:01:01G	06:02:01G	762	1,098
	706	B	02:07:01G	11:01:01G	46:01:01G	46:01:01G	01:02:01G	01:02:01G	59,000	377
	709	B	01:01:01G	02:01:01G	15:01:01G	49:01:01G	03:04:01G	07:01:01G	41,000	531

ART, antiretroviral therapy; CRF, circulating recombinant form; HLA, human leukocyte antigen; NA, not available; RMD, romidepsin.

Extended Table 2.

Adverse events.

	ART group (n=15)					ART+3BNC117 group (n=15)					ART+RMD group (n=13)					AR
	Participants		Mild	Mod.	Sev.	Participants		Mild	Mod.	Sev.	Participants		Mild	Mod.	Sev.	Partici
Events related to 3BNC117	*n*	%	*n*	*n*	*n*	*n*	%	*n*	*n*	*n*	*n*	%	*n*	*n*	*n*	*n*
Any	-	-	-	-	-	*6*	*40*	-	-	-	-	-	-	-	-	*7*
Fatigue	-	-	-	-	-	4	27	4	1	-	-	-	-	-	-	3
Headache	-	-	-	-	-	3	20	4	-	-	-	-	-	-	-	3
Chills	-	-	-	-	-	1	7	1	-	-	-	-	-	-	-	2
Blurred vision	-	-	-	-	-	2	13	2	-	-	-	-	-	-	-	-
Allergic rhinitis	-	-	-	-	-	1	7	1	-	-	-	-	-	-	-	-
Diarrhea	-	-	-	-	-	1	7	1	-	-	-	-	-	-	-	-
Dizziness	-	-	-	-	-	1	7	1	-	-	-	-	-	-	-	-
Dysguesia	-	-	-	-	-	1	7	1	-	-	-	-	-	-	-	-

	ART group (n=15)					ART+3BNC117 group (n=15)					ART+RMD group (n=13)					ART
	Participants		Mild	Mod.	Sev.	Participants		Mild	Mod.	Sev.	Participants		Mild	Mod.	Sev.	Partici
Hot flashes	-	-	-	-	-	-	-	-	-	-	-	-	-	-	-	1
Malaise	-	-	-	-	-	1	7	1	-	-	-	-	-	-	-	-
Nausea	-	-	-	-	-	1	7	1	-	-	-	-	-	-	-	-
Total	-	-	-	-	-	-	-	**17**	**1**	-	-	-	-	-	-	-
	Participants		Mild	Mod.	Sev.	Participants		Mild	Mod.	Sev.	Participants		Mild	Mod.	Sev.	Partici
Events related to RMD	*n*	%	*n*	*n*	*n*	*n*	%	*n*	*n*	*n*	*n*	%	*n*	*n*	*n*	*n*
Any	-	-	-	-	-	-	-	-	-	-	*12*	*92*	-	-	-	*15*
Nausea	-	-	-	-	-	-	-	-	-	-	7	54	11	3	-	10
Fatigue	-	-	-	-	-	-	-	-	-	-	6	46	8	2	-	8
Constipation	-	-	-	-	-	-	-	-	-	-	-	-	-	-	-	5
Headache	-	-	-	-	-	-	-	-	-	-	3	23	4	-	-	2
Dizziness	-	-	-	-	-	-	-	-	-	-	2	15		2	-	1
Dysgeusia	-	-	-	-	-	-	-	-	-	-	2	15	2	-	-	1
Abdominal pain	-	-	-	-	-	-	-	-	-	-	-	-	-	-	-	3
Anosmia	-	-	-	-	-	-	-	-	-	-	1	8	1	-	-	-
Anxiety	-	-	-	-	-	-	-	-	-	-	-	-	-	-	-	1
Chills	-	-	-	-	-	-	-	-	-	-	1	8	2	-	-	-
Hyperhidrosis	-	-	-	-	-	-	-	-	-	-	-	-	-	-	-	1
Injection site reaction	-	-	-	-	-	-	-	-	-	-	-	-	-	-	-	1
Neutropenia	-	-	-	-	-	-	-	-	-	-	-	-	-	-	-	1
Reflux gastroesophageal reflux disease	-	-	-	-	-	-	-	-	-	-	-	-	-	-	-	1
Thrombocytopeni	-	-	-	-	-	-	-	-	-	-	-	-	-	-	-	1
Total	-	-	-	-	-	-	-	-	-	-	-	-	**28**	**7**	-	-
	Participants		Mild	Mod.	Sev.	Participants		Mild	Mod.	Sev.	Participants		Mild	Mod.	Sev.	Partici
Unrelated Events	*n*	%	*n*	*n*	*n*	*n*	%	*n*	*n*	*n*	*n*	%	*n*	*n*	*n*	*n*
Any	*14*	*93*	-	-	-	*13*	*87*	-	-	-	*12*	*92*	-	-	-	*15*
Sexually transmitted infection	6	40	-	11	-	3	20	-	3	-	4	31	-	5	-	5
Headache	3	20	2	1	-	2	13	2	-	-	1	8	2	-	-	4
Upper respiratory tract infection	2	13	1	1	-	1	7	2	-	-	3	23	4	-	-	4
Nausea	1	7	1	-	-	3	20	2	1	-	2	15	1	1	-	3
Fatigue	2	13	2	2	-	1	7	1	-	-	-	-	-	-	-	5
Skin infection	2	13	1	3	-	2	13	1	1	-	2	15	1	1	-	2
Constipation	3	20	3	-	-	-	-	-	-	-	2	15	2	-	-	2
Abdominal pain	5	33	5	-	-	1	7	1	-	-	1	8	-	1	-	-
Pharyngitis	2	13	2	-	-	1	7	2	-	-	1	8	1	-	-	2

	ART group (n=15)					ART+3BNC117 group (n=15)					ART+RMD group (n=13)					AR
	Participants		Mild	Mod.	Sev.	Participants		Mild	Mod.	Sev.	Participants		Mild	Mod.	Sev.	Partici
Abdominal distension	3	20	3	-	-	-	-	-	-	-	-	-	-	-	-	2
Insomnia	2	13	2	-	-	1	7	-	1	-	-	-	-	-	-	2
Arthralgia	3	20	3	-	-	-	-	-	-	-	1	8	2	-	-	-
Myalgia	-	-	-	-	-	2	13	1	1	-	-	-	-	-	-	2
Paresthesia	1	7	1	-	-	-	-	-	-	-	1	8	1	-	-	2
Vasovagal reaction	-	-	-	-	-	1	7	1	-	-	2	15	2	-	-	1
Anxiety	1	7	1	-	-	-	-	-	-	-	1	8	1	-	-	1
Back pain	-	-	-	-	-	-	-	-	-	-	1	8	1	-	-	2
Diarrhea	2	13	2	1	-	-	-	-	-	-	-	-	-	-	-	1
Dyspnea	-	-	-	-	-	2	13	1	1	-	1	8	-	1	-	-
Eczema	-	-	-	-	-	1	7	1	-	-	-	-	-	-	-	2
Eye pain	-	-	-	-	-	-	-	-	-	-	-	-	-	-	-	3
Hyperhidrosis	-	-	-	-	-	1	7	2	-	-	1	8	1	-	-	1
Pruritus	1	7	1	-	-	1	7	1	-	-	-	-	-	-	-	1
Reflux gastroesophageal reflux disease	1	7	1	-	-	1	7	1	-	-	1	8	1	-	-	-
Thrush	1	7	-	1	-	-	-	-	-	-	-	-	-	-	-	2
Weight gain	1	7	1	-	-	-	-	-	-	-	-	-	-	-	-	2
Eye infection	1	7	-	1	-	1	7	1	-	-	-	-	-	-	-	-
Dizziness	-	-	-	-	-	2	13	2	-	-	-	-	-	-	-	-
Dry skin	-	-	-	-	-	-	-	-	-	-	-	-	-	-	-	2
Ear pain	1	7	-	1	-	1	7	1	-	-	-	-	-	-	-	-
Enterocolitis infectious	1	7	1	-	-	-	-	-	-	-	1	8	1	-	-	-
Otitis externa	1	7	-	1	-	-	-	-	-	-	-	-	-	-	-	1
Proctitis	1	7	1	-	-	1	7	1	-	-	-	-	-	-	-	-
Tinnitus	1	7	1	-	-	1	7	1	-	-	-	-	-	-	-	-
Alanine transaminase increased	-	-	-	-	-	-	-	-	-	-	-	-	-	-	-	1
Alopecia	-	-	-	-	-	1	7	1	-	-	-	-	-	-	-	-
Amnesia	-	-	-	-	-	-	-	-	-	-	1	8	1	-	-	-
Anorexia	-	-	-	-	-	-	-	-	-	-	1	8	1	-	-	-
Appendicitis	-	-	-	-	-	-	-	-	-	-	-	-	-	-	-	1
Basal cell cacinoma	-	-	-	-	-	-	-	-	-	-	-	-	-	-	-	1
Bloodstream infection	-	-	-	-	-	1	7	-	-	1	-	-	-	-	-	-
Chills	-	-	-	-	-	-	-	-	-	-	1	8	1	-	-	-
Cholecystitis	-	-	-	-	-	-	-	-	-	-	1	8	-	1	-	-
Confusion	1	7	1	-	-	-	-	-	-	-	-	-	-	-	-	-

	ART group (n=15)					ART+3BNC117 group (n=15)					ART+RMD group (n=13)					AR
	Participants		Mild	Mod.	Sev.	Participants		Mild	Mod.	Sev.	Participants		Mild	Mod.	Sev.	Partici
Dehydratio	-	-	-	-	-	1	7	1	-	-	-	-	-	-	-	-
Dry mouth	1	7	1	-	-	-	-	-	-	-	-	-	-	-	-	-
Epistaxis	-	-	-	-	-	1	7	1	-	-	-	-	-	-	-	-
Hypertension	-	-	-	-	-	-	-	-	-	-	-	-	-	-	-	1
Lung infection	-	-	-	-	-	1	7	-	1	-	-	-	-	-	-	-
Mental and behavioural disorder due to multiple drug use	-	-	-	-	-	-	-	-	-	-	1	8	-	-	1	-
Mucosal infection	-	-	-	-	-	-	-	-	-	-	-	-	-	-	-	1
Mucositis oral	-	-	-	-	-	-	-	-	-	-	1	8	1	-	-	-
Pain in extremity	-	-	-	-	-	1	7	-	1	-	-	-	-	-	-	-
Pregnancy	-	-	-	-	-	-	-	-	-	-	-	-	-	-	1	-
Radiculitis	-	-	-	-	-	-	-	-	-	-	-	-	-	-	-	-
Removal of mole	-	-	-	-	-	-	-	-	-	-	-	-	-	-	-	1
Suicide attempt	-	-	-	-	-	-	-	-	-	-	1	8	-	-	1	-
Vitamine D deficiency	-	-	-	-	-	-	-	-	-	-	-	-	-	-	-	1
Vomiting	-	-	-	-	-	-	-	-	-	-	-	-	-	-	-	1
Watering eyes	1	7	-	1	-	-	-	-	-	-	-	-	-	-	-	-
Total	-	-	**37**	**24**	-	-	-	**28**	**10**	**1**	-	-	**25**	**10**	**3**	-

Data are n for number(s) of event(s), and n (%) for the number(s) of affected participants. Events are classed according to the Common Terminology Criteria for Adverse Events (CTCAE), version 5.0 by the study physicians.

Supplementary Material

Refer to Web version on PubMed Central for supplementary material.

Acknowledgments

We thank all study participants who devoted time to our research as well as every clinical research unit involved in the study. We acknowledge Rockefeller University for providing 3BNC117, Bristol-Myers Squibb Company (Celgene Corporation) for providing the romidepsin as well as the Labcorp-Monogram Biosciences Clinical Reference Laboratory for performing the phenotypic resistance assays with project management from Yolanda Lie and Charles Kang. Finally, we would like to acknowledge the amazing support and help by the late Amin Alamshah, a kind and brilliant clinical project manager for the Imperial College Centre for Translational and Experimental Medicine, who tragically lost his life prior to the completion of this study. The funders were neither involved in the study design/operations, data collection/analysis/interpretation nor preparation of the manuscript.

Financial Support

Funded by the Danish Council for Independent Research (grants #7016-00022 and #9060-00023B OSS), Central Region Denmark Research Fund, The Danish Regions' Medicine and Treatment Fund, Aarhus University, and Next Experimental Therapy Partnership. Research reported in this publication was also supported by the National Institute Of Allergy And Infectious Diseases of the National Institutes of Health (Award Number #UM1AI164565 RBJ). The content is solely the responsibility of the authors and does not necessarily represent the official views of the National Institutes of Health. A Vanier Award from the Canadian Institutes for Health Research (NNK). A scholar award from the Michael Smith Foundation for Health Research (ZLB). Study drugs were donated free of charge by The Rockefeller University (3BNC117) and Celgene (romidepsin) for use in this trial. None of the

specific sources of funding had any role in the conceptualization, design, data collection, analysis, decision to publish, or preparation of the manuscript.

Data availability

Data are not available for download due to privacy/ethical restrictions under the EU GDPR. Specific requests for access to the trial data may be sent to olesoega@rm.dk and access may be provided to a named individual in agreement with the rules and regulations of the Danish Data Protection agency and the National Committee on Health Research Ethics with a 2-week response time-frame to requests.

References

1. Abrahams MR et al. The replication-competent HIV-1 latent reservoir is primarily established near the time of therapy initiation. Sci. Transl. Med 11, (2019).
2. Brodin J et al. Establishment and stability of the latent HIV-1 DNA reservoir. Elife 5, 1–14 (2016).
3. Martin GE et al. Levels of Human Immunodeficiency Virus DNA Are Determined Before ART Initiation and Linked to CD8 T-Cell Activation and Memory Expansion. J. Infect. Dis 1–11 (2019). doi:10.1093/infdis/jiz563
4. Jones BR et al. Phylogenetic approach to recover integration dates of latent HIV sequences within-host. Proc. Natl. Acad. Sci. U. S. A 115, E8958–E8967 (2018). [PubMed: 30185556]
5. Brooks K et al. HIV-1 variants are archived throughout infection and persist in the reservoir. PLoS Pathog. 16, 1–22 (2020).
6. Rasmussen TA et al. Panobinostat, a histone deacetylase inhibitor, for latent-virus reactivation in HIV-infected patients on suppressive antiretroviral therapy: a phase 1/2, single group, clinical trial. lancet. HIV 1, e13–21 (2014). [PubMed: 26423811]
7. Li JZ et al. The size of the expressed HIV reservoir predicts timing of viral rebound after treatment interruption. AIDS 30, 1 (2015).
8. Kroon EDMB et al. A randomized trial of vorinostat with treatment interruption after initiating antiretroviral therapy during acute HIV-1 infection. J. Virus Erad 6, 0–7 (2020).
9. Leth S et al. Combined effect of Vacc-4x, recombinant human granulocyte macrophage colony-stimulating factor vaccination, and romidepsin on the HIV-1 reservoir (REDUC): a single-arm, phase 1B/2A trial. Lancet HIV 3, e463–e472 (2016). [PubMed: 27658863]
10. Gruell H et al. Effect of 3BNC117 and romidepsin on the HIV-1 reservoir in people taking suppressive antiretroviral therapy (ROADMAP): a randomised, open-label, phase 2A trial. The Lancet Microbe 5247, 1–12 (2022).
11. Søgaard OS et al. The Depsipeptide Romidepsin Reverses HIV-1 Latency In Vivo. PLoS Pathog. 11, e1005142 (2015). [PubMed: 26379282]
12. Lehrman G et al. Depletion of latent HIV-1 infection in vivo: a proof-of-concept study. Lancet 366, 549–555 (2005). [PubMed: 16099290]
13. Archin NM et al. Valproic acid without intensified antiviral therapy has limited impact on persistent HIV infection of resting CD4+ T cells. AIDS 22, 1131–1135 (2008). [PubMed: 18525258]
14. Archin NM et al. Antiretroviral intensification and valproic acid lack sustained effect on residual HIV-1 viremia or resting CD4+ cell infection. PLoS One 5, e9390 (2010). [PubMed: 20186346]
15. Routy JP et al. Design and Implementation of a Randomized Crossover Study of Valproic Acid and Antiretroviral Therapy to Reduce the HIV Reservoir. HIV Clin. Trials 13, 301–307 (2012). [PubMed: 23195668]
16. Archin NM et al. Administration of vorinostat disrupts HIV-1 latency in patients on antiretroviral therapy. Nature 487, 482–5 (2012). [PubMed: 22837004]
17. Elliott JH et al. Activation of HIV Transcription with Short-Course Vorinostat in HIV-Infected Patients on Suppressive Antiretroviral Therapy. PLoS Pathog. 10, e1004473 (2014). [PubMed: 25393648]

18. Archin NM et al. HIV-1 Expression Within Resting CD4+ T Cells After Multiple Doses of Vorinostat. J. Infect. Dis 210, 728–735 (2014). [PubMed: 24620025]
19. Wei DG et al. Histone Deacetylase Inhibitor Romidepsin Induces HIV Expression in CD4 T Cells from Patients on Suppressive Antiretroviral Therapy at Concentrations Achieved by Clinical Dosing. PLoS Pathog. 10, e1004071 (2014). [PubMed: 24722454]
20. Gunst JD, Tolstrup M, Rasmussen TA & Søgaard OS The potential role for romidepsin as a component in early HIV-1 curative efforts. Expert Rev. Anti. Infect. Ther 14, 447–450 (2016). [PubMed: 26953620]
21. McMahon DK et al. A Phase 1/2 Randomized, Placebo-Controlled Trial of Romidespin in Persons With HIV-1 on Suppressive Antiretroviral Therapy. J. Infect. Dis 224, 648–656 (2021). [PubMed: 34398236]
22. Shan L et al. Stimulation of HIV-1-Specific Cytolytic T Lymphocytes Facilitates Elimination of Latent Viral Reservoir after Virus Reactivation. Immunity 36, 491–501 (2012). [PubMed: 22406268]
23. Mothe B et al. HIVconsv Vaccines and Romidepsin in Early-Treated HIV-1-Infected Individuals: Safety, Immunogenicity and Effect on the Viral Reservoir (Study BCN02). Front. Immunol 11, 1–15 (2020). [PubMed: 32038653]
24. Fidler S et al. Antiretroviral therapy alone versus antiretroviral therapy with a kick and kill approach, on measures of the HIV reservoir in participants with recent HIV infection (the RIVER trial): a phase 2, randomised trial. Lancet 6736, 1–11 (2020).
25. Caskey M, Klein F & Nussenzweig MC Broadly neutralizing anti-HIV-1 monoclonal antibodies in the clinic. Nat. Med 25, 547–553 (2019). [PubMed: 30936546]
26. Lu C-L et al. Enhanced clearance of HIV-1–infected cells by broadly neutralizing antibodies against HIV-1 in vivo. Science (80-.). 352, 1001–1004 (2016).
27. Dufloo J et al. Broadly neutralizing anti-HIV-1 antibodies tether viral particles at the surface of infected cells. Nat. Commun 13, 1–11 (2022). [PubMed: 34983933]
28. Schoofs T et al. HIV-1 therapy with monoclonal antibody 3BNC117 elicits host immune responses against HIV-1. Science 0972, (2016).
29. Niessl J et al. Combination anti-HIV-1 antibody therapy is associated with increased virus-specific T cell immunity. Nat. Med 26, 222–227 (2020). [PubMed: 32015556]
30. Scheid JF et al. Sequence and structural convergence of broad and potent HIV antibodies that mimic CD4 binding. Science 333, 1633–7 (2011). [PubMed: 21764753]
31. Nishimura Y et al. Early antibody therapy can induce long-lasting immunity to SHIV. Nature 543, 559–563 (2017). [PubMed: 28289286]
32. DiLillo DJ & Ravetch JV Differential Fc-receptor engagement drives an anti-tumor vaccinal effect. Cell 161, 1035–1045 (2015). [PubMed: 25976835]
33. Gay CL et al. Stable Latent HIV Infection and Low-level Viremia Despite Treatment With the Broadly Neutralizing Antibody VRC07-523LS and the Latency Reversal Agent Vorinostat. J. Infect. Dis 1–25 (2021). doi:10.1093/infdis/jiab487
34. Gunst JD, Tolstrup M & Søgaard OS Beyond antiretroviral therapy: early interventions to control HIV-1 infection. AIDS 31, 1665–1667 (2017). [PubMed: 28463884]
35. Reece J et al. An ‘escape clock’ for estimating the turnover of SIV DNA in resting CD4+ T cells. PLoS Pathog. 8, e1002615 (2012). [PubMed: 22496643]
36. Reece JC et al. Measuring Turnover of SIV DNA in Resting CD4+ T Cells Using Pyrosequencing: Implications for the Timing of HIV Eradication Therapies. PLoS One 9, e93330 (2014). [PubMed: 24710023]
37. Petravic J, Martyushev A, Reece JC, Kent SJ & Davenport MP Modeling the Timing of Antilatency Drug Administration during HIV Treatment. J. Virol 88, 14050–14056 (2014). [PubMed: 25253352]
38. Baxter AE et al. Multiparametric characterization of rare HIV-infected cells using an RNA-flow FISH technique. Nat. Protoc 12, 2029–2049 (2017). [PubMed: 28880280]
39. Puertas MC et al. VIP-SPOT: an Innovative Assay To Quantify the Productive HIV-1 Reservoir in the Monitoring of Cure Strategies. MBio 12, (2021).

40. Bruner KM et al. A quantitative approach for measuring the reservoir of latent HIV-1 proviruses. Nature 566, 120–125 (2019). [PubMed: 30700913]
41. Kinloch NN et al. HIV-1 diversity considerations in the application of the Intact Proviral DNA Assay (IPDA). Nat. Commun 12, 165 (2021). [PubMed: 33420062]
42. Caskey M et al. Viraemia suppressed in HIV-1-infected humans by broadly neutralizing antibody 3BNC117. Nature 522, 487–491 (2015). [PubMed: 25855300]
43. Bar-On Y et al. Safety and antiviral activity of combination HIV-1 broadly neutralizing antibodies in viremic individuals. Nat. Med 24, 1701–1707 (2018). [PubMed: 30258217]
44. Stephenson KE et al. Safety, pharmacokinetics and antiviral activity of PGT121, a broadly neutralizing monoclonal antibody against HIV-1: a randomized, placebo-controlled, phase 1 clinical trial. Nat. Med 27, 1718–1724 (2021). [PubMed: 34621054]
45. Caskey M et al. Antibody 10-1074 suppresses viremia in HIV-1-infected individuals. Nat. Med 23, 185–191 (2017). [PubMed: 28092665]
46. Feng Q et al. Quadruple versus triple combination antiretroviral therapies for treatment naive people with HIV: Systematic review and meta-analysis of randomised controlled trials. BMJ 366, (2019).
47. Markowitz M et al. A Randomized Open-Label Study of 3- Versus 5-Drug Combination Antiretroviral Therapy in Newly HIV-1-Infected Individuals. JAIDS J. Acquir. Immune Defic. Syndr 66, 140–147 (2014). [PubMed: 24457632]
48. Scheid JF et al. Sequence and Structural Convergence. Science 333, 1633–1637 (2011). [PubMed: 21764753]
49. Stefic K, Bouvin-Pley M, Braibant M & Barin F Impact of HIV-1 diversity on its sensitivity to neutralization. Vaccines 7, 1–14 (2019).
50. Wang P et al. Quantifying the contribution of Fc-mediated effector functions to the antiviral activity of anti–HIV-1 IgG1 antibodies in vivo. Proc. Natl. Acad. Sci. U. S. A 117, 18002–18009 (2020). [PubMed: 32665438]
51. Asokan M et al. Fc-mediated effector function contributes to the in vivo antiviral effect of an HIV neutralizing antibody. Proc. Natl. Acad. Sci. U. S. A 117, 18754–18763 (2020). [PubMed: 32690707]
52. Veenhuis RT, Garliss CC, Bailey JR & Blankson JN CD8 Effector T Cells Function Synergistically With Broadly Neutralizing Antibodies to Enhance Suppression of HIV Infection. Front. Immunol 12, 1–10 (2021).
53. Spencer DA et al. Phagocytosis by an HIV antibody is associated with reduced viremia irrespective of enhanced complement lysis. Nat. Commun 13, 1–14 (2022). [PubMed: 34983933]
54. Chomont N et al. HIV reservoir size and persistence are driven by T cell survival and homeostatic proliferation. Nat. Med 15, 893–900 (2009). [PubMed: 19543283]
55. Hiener B et al. Identification of Genetically Intact HIV-1 Proviruses in Specific CD4 + T Cells from Effectively Treated Participants. Cell Rep. 21, 813–822 (2017). [PubMed: 29045846]
56. Buzon MJ et al. HIV-1 persistence in CD4(+) T cells with stem cell-like properties. Nat. Med 20, 139–142 (2014). [PubMed: 24412925]
57. Jaafoura S et al. Progressive contraction of the latent HIV reservoir around a core of less-differentiated CD4 + memory T cells. Nat. Commun 5, (2014).
58. Collins DR, Gaiha GD & Walker BD CD8+ T cells in HIV control, cure and prevention. Nat. Rev. Immunol 20, 471–482 (2020). [PubMed: 32051540]
59. Mendoza P et al. Combination therapy with anti-HIV-1 antibodies maintains viral suppression. Nature 561, 479–484 (2018). [PubMed: 30258136]
60. Deeks SG et al. Research priorities for an HIV cure: International AIDS Society Global Scientific Strategy 2021. Nat. Med 27, 2085–2098 (2021). [PubMed: 34848888]

References for Methods

61. Estes JD et al. Defining total-body AIDS-virus burden with implications for curative strategies. Nat. Med (2017). doi:10.1038/nm.4411

62. Gaebler C et al. Prolonged viral suppression with anti-HIV-1 antibody therapy. Nature (2022). doi:10.1038/s41586-022-04597-1
63. Schulz KF, Altman DG & Moher D CONSORT 2010 Statement: Updated guidelines for reporting parallel group randomised trials. Trials (2010). doi:10.1186/1745-6215-11-32
64. Harris P. a. et al. Research electronic data capture (REDCap)-A metadata-driven methodology and workflow process for providing translational research informatics support. J. Biomed. Inform 42, 377–381 (2009). [PubMed: 18929686]
65. Harris PA et al. The REDCap consortium: Building an international community of software platform partners. Journal of Biomedical Informatics (2019). doi:10.1016/j.jbi.2019.103208
66. Bar-On Y et al. Safety and antiviral activity of combination HIV-1 broadly neutralizing antibodies in viremic individuals. Nat. Med (2018). doi:10.1038/s41591-018-0186-4
67. Baxter AE et al. Single-Cell Characterization of Viral Translation-Competent Reservoirs in HIV-Infected Individuals. Cell Host Microbe 20, 368–380 (2016). [PubMed: 27545045]
68. Grau-Expósito J et al. A Novel Single-Cell FISH-Flow Assay Identifies Effector Memory CD4 + T cells as a Major Niche for HIV-1 Transcription in HIV-Infected Patients. MBio 8, e00876–17 (2017). [PubMed: 28698276]
69. Gaebler C et al. Combination of quadruplex qPCR and next-generation sequencing for qualitative and quantitative analysis of the HIV-1 latent reservoir. J. Exp. Med (2019). doi:10.1084/jem.20190896
70. Parekh BS et al. Performance evaluation of AsanteTM Rapid Recency Assay for HIV diagnosis and detection of recent infection: potential for surveillance and prevention. in 9th IAS Conference on HIV Science in Paris, France (2017).
71. Julg B et al. Recommendations for analytical antiretroviral treatment interruptions in HIV research trials—report of a consensus meeting. Lancet HIV 6, e259–e268 (2019). [PubMed: 30885693]
72. Besson GJ et al. HIV-1 DNA Decay Dynamics in Blood During More Than a Decade of Suppressive Antiretroviral Therapy. Clin. Infect. Dis 59, (2014).
73. Royston P Multiple imputation of missing values: Further update of ice, with an emphasis on categorical variables. Stata J. 9, 466–477 (2009).
74. Rubin DB Multiple Imputation for Nonresponse in Surveys. (Wiley, 2004).
75. Austin PC, White IR, Lee DS & van Buuren S Missing Data in Clinical Research: A Tutorial on Multiple Imputation. Can. J. Cardiol 37, 1322–1331 (2021 [PubMed: 33276049]

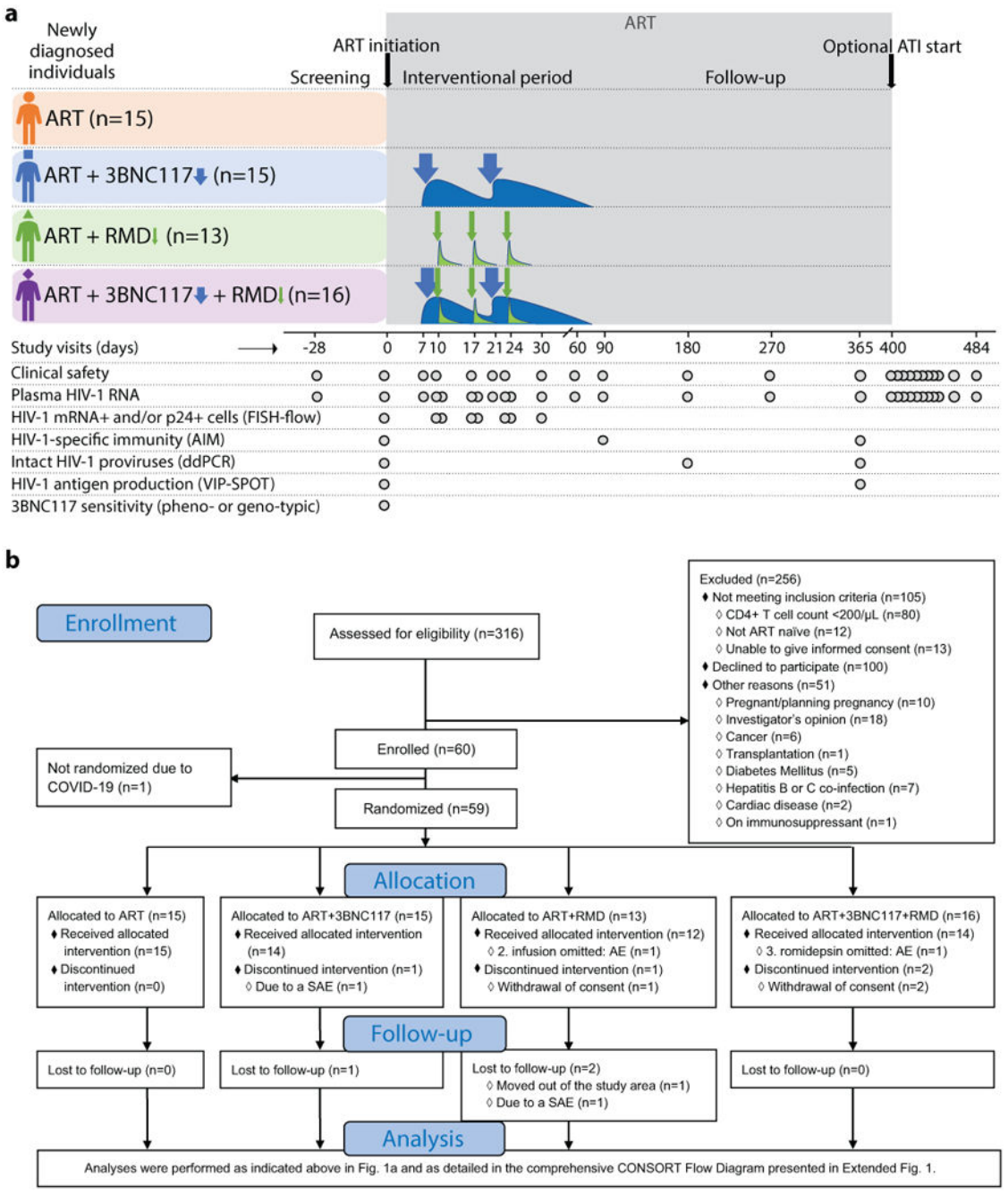

Figure 1. The eCLEAR trial design (a) and abbreviated CONSORT Flow Diagram (b).

The Analysis section is presented in full in Extended Fig. 1.

AIM, activation-induced marker; ART, antiretroviral therapy; ATI, analytical treatment interruption; COVID-19, coronavirus disease 2019; ddPCR, droplet digital polymerase chain reaction; FISH, fluorescence in situ hybridization; RMD, romidepsin; VIP-SPOT, viral protein spot.

a

	Participant ID	Subtype	Monogram PhenoSense IC90	Monogram PhenoSense MPI	*Env* sequencing Sensitive/ total	Assessment
ART+3BNC117 (n=15)	109	D	-	-	33/33	Sensitive
	135	CRF01	-	-	31/31	Sensitive
	210	B	0.62	98.0	-	Sensitive
	211	B	-	-	48/51	Sensitive
	302	CRF01	0.66	99.8	-	Sensitive
	412	B	0.18	99.5	-	Sensitive
	701	B	0.92	99.7	-	Sensitive
	703	CRF02	0.30	99.9	-	Sensitive
	106	CRF01	2.48	99.1	-	Resistant
	125	B	1.63	97.2	-	Resistant
	126	CRF01	2.10	97.8	-	Resistant
	205	B	3.41	97.0	-	Resistant
	401	B	4.15	98.2	-	Resistant
	404	A	1.88	99.0	-	Resistant
	704	CRF01	>50	44.2	-	Resistant
ART+3BNC117+RMD (n=16)	103	B	0.96	99.2	-	Sensitive
	107	CRF01	0.25	99.9	-	Sensitive
	116	C	0.34	99.9	-	Sensitive
	130	CRF01	-	-	33/33	Sensitive
	203	CRF01	1.22	99.6	-	Sensitive
	212	CRF47	0.67	99.9	-	Sensitive
	303	CRF02	0.20	99.6	-	Sensitive
	304	B	0.74	99.9	-	Sensitive
	408	B	0.15	99.5	-	Sensitive
	706	B	0.80	99.7	-	Sensitive
	112	G	>50	08.6	-	Resistant
	301	B	4.51	98.8	-	Resistant
	308	CRF01	3.09	94.6	-	Resistant
	402	B	-	-	7/35	Resistant
	411	B	3.22	99.3	-	Resistant
	709	B	7.44	96.3	-	Resistant

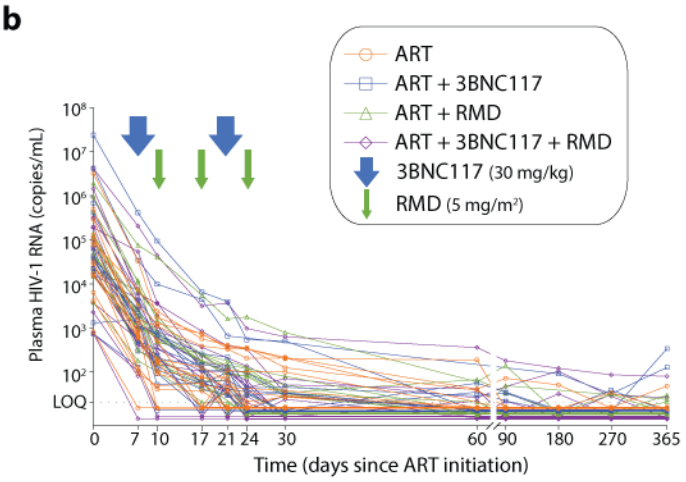

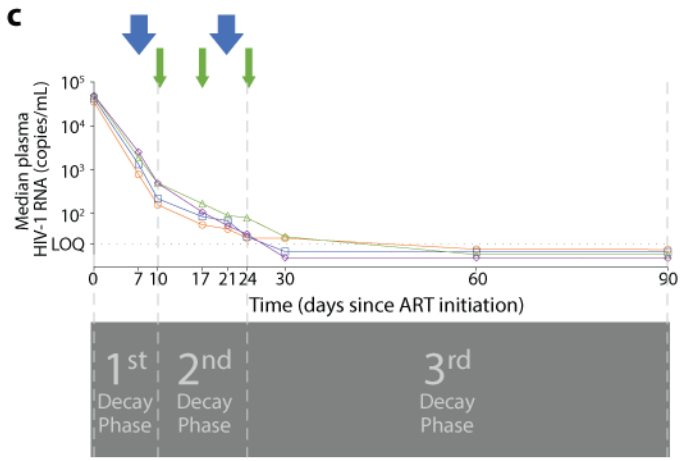

d

Median daily decay in plasma HIV-1 RNA (%)	Decay Phase (days)		1st (0-10)	95%-CI	*P*	2nd (10-24)	95%-CI	*P*	3rd (24-90)	95%-CI	*P*
	Overall	ART	-41.1	(-55.2;-22.7)	ref	-10.0	(-14.9;-4.86)	ref	-3.19	(-4.75;-1.61)	ref
		ART+3BNC117	-43.7	(-71.1;9.66)	0.823	-16.4	(-27.0;-4.29)	0.070	-3.09	(-6.54;0.49)	0.918
		ART+RMD	-36.2	(-67.5;25.2)	0.694	-18.5	(-29.0;-6.51)	0.017	-3.03	(-6.54;0.61)	0.875
		ART+3BNC117+RMD	-36.5	(-67.3;23.2)	0.706	-16.9	(-27.3;-4.93)	0.048	-2.70	(-6.19;0.92)	0.622
	Sensitive	ART+3BNC117	-38.9	(-62.1;-1.41)	0.714	-17.9	(-28.8;-5.16)	0.045	-4.02	(-7.80;-0.07)	0.488
		ART+3BNC117+RMD	-36.2	(-60.1;1.91)	0.556	-17.9	(-28.8;-5.28)	0.042	-2.81	(-6.64;1.17)	0.739
	Resistant	ART+3BNC117	-48.8	(-69.0;-15.5)	0.629	-14.7	(-26.0;-1.58)	0.247	-2.02	(-5.87;1.98)	0.327
		ART+3BNC117+RMD	-37.0	(-61.7;3.39)	0.631	-15.1	(-26.2;-2.28)	0.198	-2.51	(-6.48;1.64)	0.568

Figure 2. 3BNC117-sensitivity at baseline and median decay of plasma HIV-1 RNA levels following ART initiation.

3BNC117-sensitivity at baseline for the ART+3BNC117 (n=15) and ART+3BNC117+RMD (n=16) groups (**a**). Individual (**b**) and group median (**c**) decay of plasma HIV-1 RNA levels following ART initiation. The arrows represent 3BNC117 and RMD infusion time points. The horizontal dotted line represents the limit of quantification (LOQ) at 20 copies/mL of the clinical HIV-1 viral load assay. The four vertical dotted lines at days 0, 10, 24 and 90 after ART initiation indicate the three plasma HIV-1 RNA decay phases (1st phase: 0-10 days; 2nd phase: 10-24 days; and 3rd phase: 24-90 days) (**c**). The percentage decline

in median plasma HIV-1 RNA levels per day is presented during the three decay phases following ART initiation in the four randomization groups as well as in groups based on 3BNC117-sensitivity (**d**). *P* values calculated using mixed-effects linear regression models with a random effect for individual participants. We considered a two-sided α value of less than 0.05 significant with no adjustments made for multiple comparisons.
ART, antiretroviral therapy; *env*, HIV-1 envelope gene; IC90, concentration of 3BNC117 required to inhibit viral replication by 90%; LOQ, limit of quantification; MPI, % inhibition observed at the highest concentration of 3BNC117 tested; RMD, romidepsin.

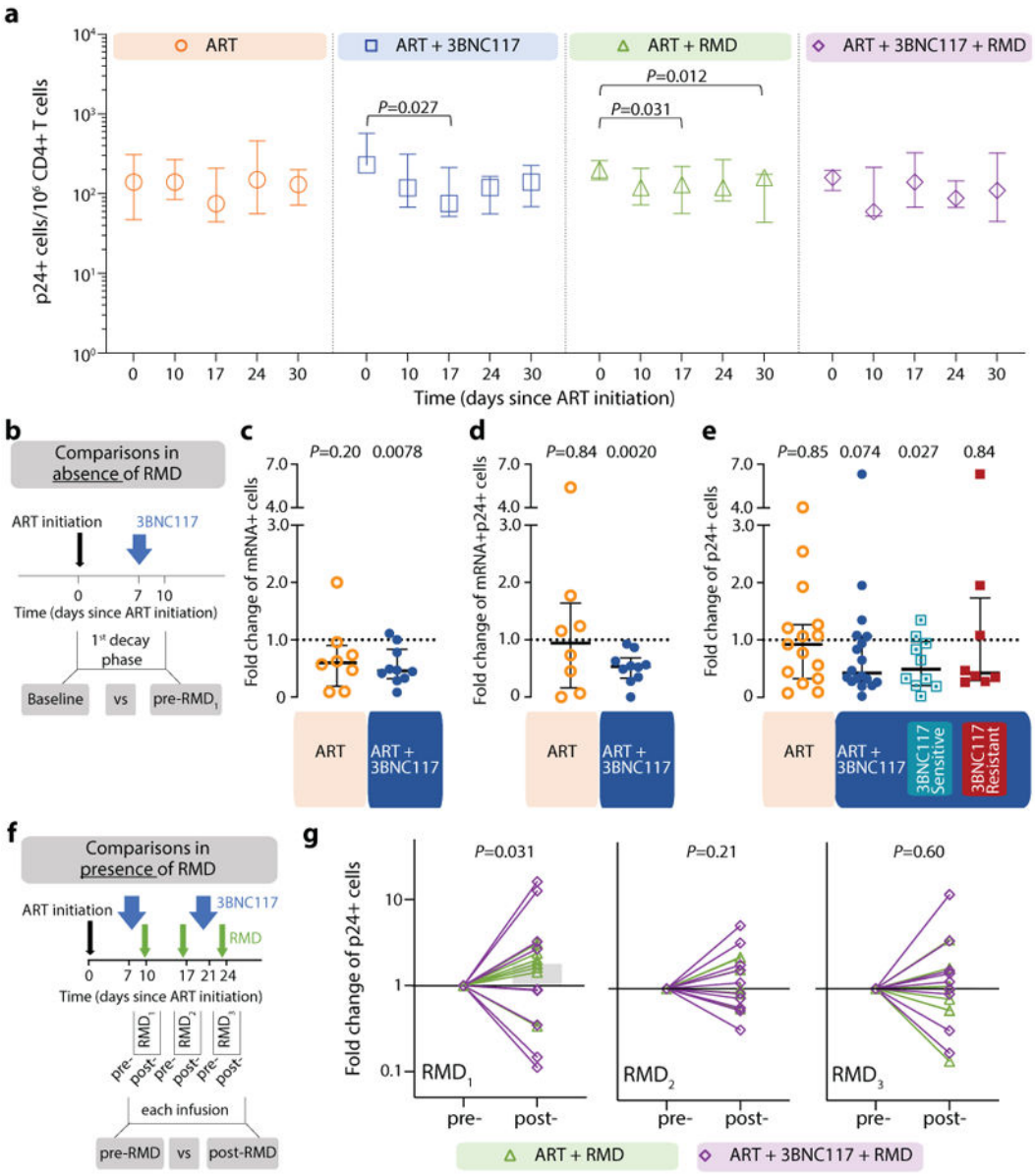

Figure 3. Transcriptionally and/or translationally active HIV-1-infected cells following ART initiation.

Changes in HIV-1-infected cells during the first 30 days of ART among the four groups shown as median (error bars represent interquartile ranges) number of CD3+CD8− T cells expressing Gag p24 protein/10^6 CD4+ T cells (**a**, ART n=7, ART+3BNC117 n=9, ART+RMD n=9, ART+3BNC117+RMD n=10). Effect of 3BNC117 on transcriptionally and/or translationally HIV-1-infected cells from baseline to day 10 – the first decay phase defined in Figure 2c (**b-e**). The schematic illustration shows how data was combined from the ART only and ART+RMD groups (who only received ART during the first 10 days) compared to the two 3BNC117-treated groups (**b**). Median (IQR) fold change in CD3+CD8− T cells expressing either HIV-1 mRNA (**c**; ART n=8, ART+3BNC117 n=10), mRNA and p24 (**d**; ART n=8, ART+3BNC117 n=10), or p24 (**e**; ART n=15, ART+3BNC117 n=18) among the combined ART and ART+3BNC117 groups, and with the

ART+3BNC117 group categorized according to 3BNC117-sensitivity (sensitive n=10 versus resistant n=8) (**e**). Due to a faulty mRNA probe in the 2nd batch of fluorescence in situ hybridization-flow cytometry analyses, mRNA data was only available for half of the study population (**c-d**). The schematic illustration shows how we analyzed the pre- to post-infusion effect of RMD on the translationally active HIV-1-infected cells (**f**). Individual and overall median fold change (gray column) from pre- to post-RMD infusions [overall median (IQR) for RMD_1 1.78 (0.61-3.09), RMD_2 1.00 (0.68-2.09), and RMD_3 1.03 (0.56-1.70)] in groups ART+RMD (n=8) and ART+3BNC117+RMD (n=10) on CD3+CD8− T cells expressing p24 (**g**). *P* values comparing within group and between groups were calculated using paired two-tailed Wilcoxon test and two-tailed Mann-Whitney test, respectively.
ART, antiretroviral therapy; IQR, interquartile ranges; RMD, romidepsin.

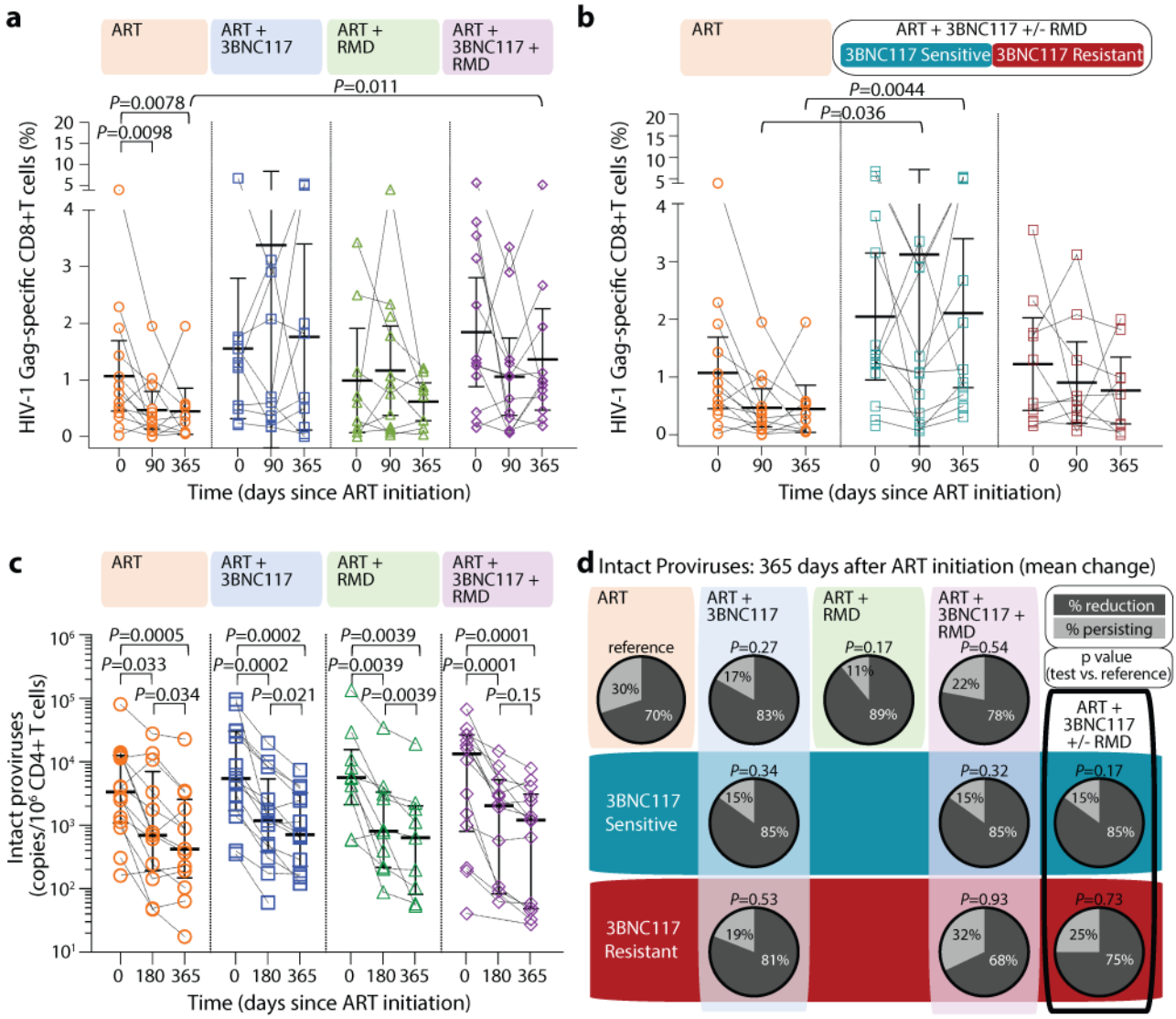

Figure 4. HIV-1 Gag-specific CD8+ T cell immunity and size of the intact HIV-1 reservoir.

Dot plot of the frequency of HIV-1 Gag-specific CD8+ T cells at ART initiation (day 0) and after 90 and 365 days of ART among the four groups (lines at median and interquartile ranges) (**a**). Dot plot of the net frequency of HIV-1 Gag-specific CD8+ T cells in groups ART+3BNC117+/−RMD categorized according to 3BNC117-sensitivity (lines at median and IQR) (**b**). The size of the intact HIV-1 reservoir at ART initiation (day 0) and after 180 and 365 days of ART among individuals in the four randomization groups (lines at median and IQR) (**c**). *P* values comparing within group and between groups were calculated using paired two-tailed Wilcoxon test and two-tailed Mann-Whitney test, respectively. Pie charts showing the mean percentage reduction of intact proviral DNA per 10^6 CD4+ T cells after 365 days of ART per group (column and upper row) and categorized according to pre-ART plasma virus sensitivity (middle row; blue shaded area) or resistance (bottom row; red shaded area) to 3BNC117 (**d**). *P* values comparing between groups were calculated using unpaired two-tailed t test with ART only as reference. A compiled group ART+3BNC117+/

−RMD is shown is the last column. ART n=14, ART+3BNC117 n=14, ART+RMD n=10, ART+3BNC117+RMD n=14.

ART, antiretroviral therapy; IQR, interquartile ranges; RMD, romidepsin; SD, standard deviation.

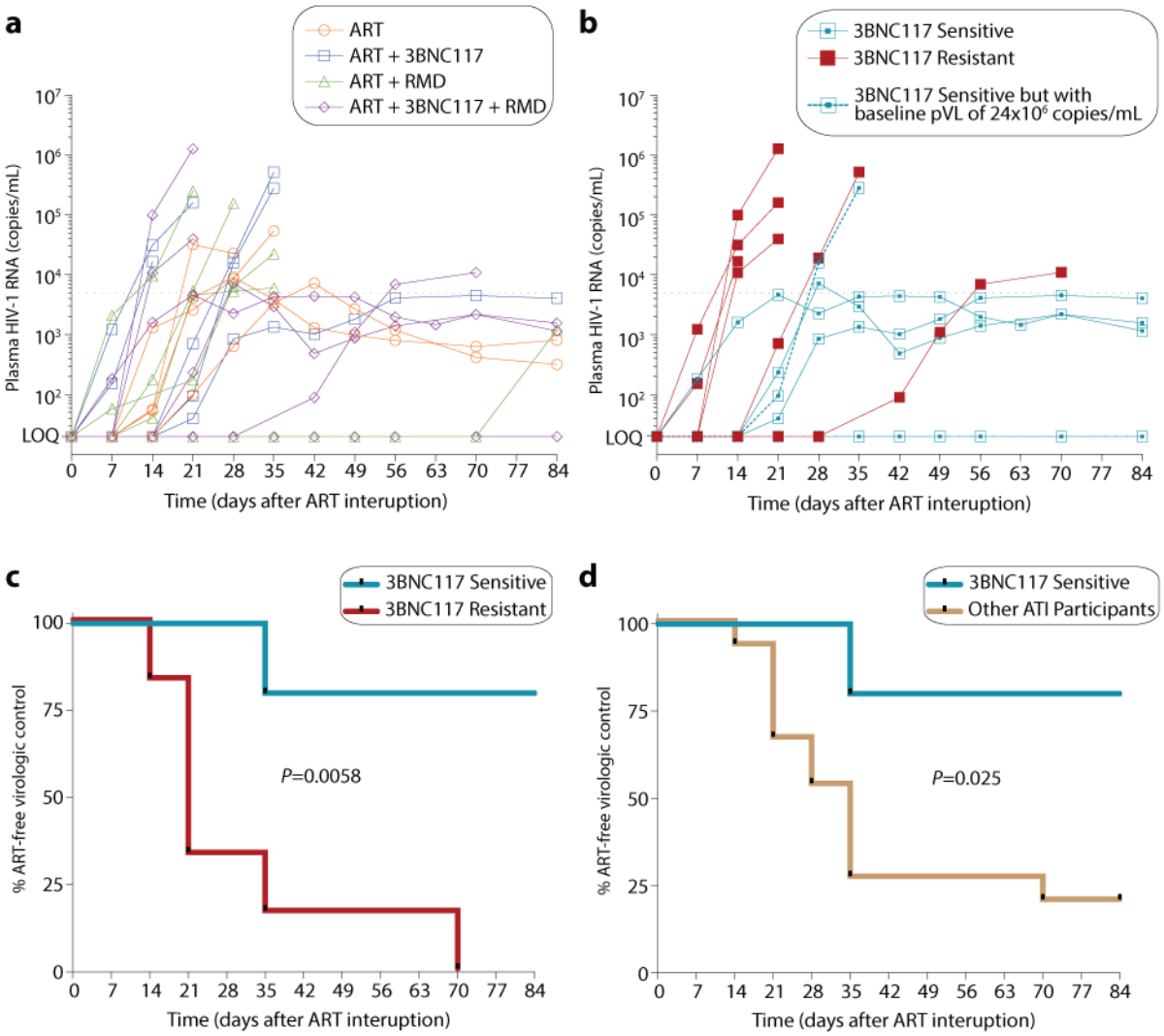

Figure 5. Time to loss of virologic control during 12 weeks of analytical treatment interruption.

Individual (n=20) plasma HIV-1 RNA levels are shown and coded by group (**a**). One individual (id. 125) resumed ART prior to fulfilling the restarting criteria due to national restrictions during the COVID-19 pandemic. Individual (n=11) plasma HIV-1 RNA levels for the ART+3BNC117 and ART+3BNC117+RMD groups based on 3BNC117-sensitivity (**b**). Kaplan-Meier curves showing percentage of individuals still interrupting ART from day 0 to day 84 during the ATI (**c-d**). Time to loss of virologic control for the ART+3BNC117 and ART+3BNC117+RMD groups based on 3BNC117-sensitivity (sensitive n=5 versus resistant n=6) (**c**) and for the 3BNC117-sensitive individuals (n=5) compared to the other ATI participants (n=15) (**d**) are shown. *P* values were calculated using log-rank test.

ART, antiretroviral therapy; ATI, analytical treatment interruption; COVID-19, coronavirus disease 2019; LOQ, limit of quantification; RMD, romidepsin.

Table 1.

Baseline characteristics for the study population.

	ART (n=15)	ART +3BNC117 (n=15)	ART +RMD (n=13)	ART +3BNC117+RMD (n=16)
Age - yr	33 (25-58)	41 (25-69)	32 (18-68)	37 (22-57)
Female sex	04 (27)	00 (00)	01 (08)	00 (00)
Race				
Asian	01 (07)	01 (07)	01 (08)	02 (13)
Black or African European	02 (13)	00 (00)	01 (08)	00 (00)
White or Caucasian	12 (80)	13 (86)	09 (69)	14 (88)
Other	00 (00)	01 (07)	02 (15)	00 (00)
Time from infection to study enrollment[§]				
Recent (<6 months)	10 (67)	04 (27)	05 (38)	09 (56)
Long-term (>6 months)	05 (33)	09 (60)	07 (54)	06 (38)
Unknown	00 (00)	02 (13)	01 (08)	01 (06)
CD4+ T cell count - cells/mm^3	560 (252-1,497)	506 (218-984)	391 (286-1,333)	531 (203-1,098)
HIV-1 RNA level - copies/ml	39.207 (820-3,240,000)	56.800 (740-24,000,000)	49.400 (3,800-1,900,000)	50.000 (730-4,180,000)
HIV-1 subtype[¥]				
B	07 (47)	07 (47)	06 (46)	08 (50)
Non-B	08 (53)	08 (53)	07 (54)	08 (50)
Human leukocyte antigen class I alleles[¥]				
Risk: B*07, B*35	06 (40)	04 (27)	04 (31)	02 (13)
Protective: B*27, B*57, B*58	03 (20)	01 (07)	02 (15)	05 (31)

Data are median (range) or n (%)

[§], Time from infection to study enrollment was self-reported.

[¥], Individual HIV-1 subtypes and human leukocyte antigen class I can be found in the Supplementary Table S1.

ART, antiretroviral therapy; COVID-19, coronavirus disease 2019; RMD, romidepsin.